THE UNIVERSITY OF WESTERN ONTARIO
DEPARTMENT OF CIVIL AND
ENVIRONMENTAL ENGINEERING

Water Resources Research Report

Integrated Reservoir Management System for Adaptation to Climate Change Impacts in the Upper Thames River Basin

By:
Hyung-Il Eum
Vasan Arunachalam
and
Slobodan P. Simonovic

Report No: 062
Date: March 2009

ISSN: (print) 1913-3200; (online) 1913-3219;
ISBN: (print) 978-0-7714-2710-7; (online) 978-0-7714-2711-4;

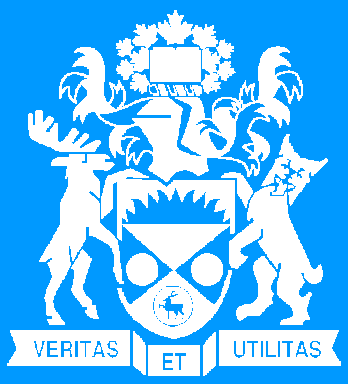

Integrated Reservoir Management System for Adaptation to Climate Change Impacts in the Upper Thames River Basin

By

Hyung-Il Eum

Vasan Arunachalam

and

Slobodan P. Simonovic

Department of Civil and Environmental Engineering

The University of Western Ontario

London, Ontario, Canada

March 2009

Executive summary

Climate change is one of the more pressing issues that attract the attention of scientists and policy makers. Many scientists are developing necessary methodologies to better understand the impacts of climate change, and support the development of appropriate adaptation measures. Literature on the application of adaptation measures to changing climatic conditions is very limited and the need for more work is evident on the development of adaptation strategies for mitigating negative impacts of climate change in water resources management practice.

This study presents an integrated reservoir management system for the Upper Thames River basin that includes: (1) a Weather Generator (WG) model; (2) a hydrologic model; and (3) a differential evolutionary optimization model. It is used to develop the alternative optimal operating rule curves for three reservoirs in the basin that will take into consideration the impact of climate change. Alternative curves developed using the proposed methodology represent one of the possible climate change adaptation strategies for the use of existing storage in the basin.

Three different weather scenarios are employed to verify the integrated reservoir management system; (1) Case 1: scenarios set I generated with the original WG model of Sharif and Burn (2006) with one variable (precipitation); (2) Case 2: scenario set II: generated with original WG model with three variables named WG3; (3) scenario set III: generated with the modified WG that is combined with Principal Component Analysis using three variables WG-PCA3. The results of this study indicate that the rule curves developed using B11(dry) climate scenario show the best result for the scenarios set I because there is no significant flood events in the case 1 and for the scenario set IIand the scenario set III generated by WG3 and WG-PCA3, the B11 (PCA) rule curves provide the best result for B11, B11(PCA), and

historic(PCA) scenarios and the B21 rule curves represent the best results for B21 and B21(PCA) scenarios. Another notable result is that the flood operations would be required until April if the B21(wet) scenario occurs in the future. In addition, the WG-PCA3 provides more wet weather conditions than the original WG model.

Contents

List of Tables

List of Figures

1. Introduction

Climate change is affecting management of water resources in different ways at different locations around the world. Our focus in this research is to assess the impact of climate change on the management of three existing reservoirs in the Upper Thames River basin, Ontario, Canada.

1.1 Background

Climate change is one of the issues that attract the attention of scientists and policy makers. Policy makers are dealing with legislation and necessary funding for mitigating the climate change and adapting to climate change impacts. On the other hand, scientists are developing necessary methodologies to better understand the impacts of climate change, and support development of appropriate adaptation measures. However, due to the large uncertainty associated to climate change impacts a very few adaptation measures have been developed and applied in practice. To alleviate the uncertainty problem, the General Circulation Models (GCMs) provide the range of feasible future scenarios employing various emission scenarios (IPCC, 2000). GCM simulation results (e.g. temperature, precipitation, wind speed, humidity, and pressure) on a global scale (IPCC, 2007) show that the Earth's average temperature will increase up to 3°C by 2080 due to the global warming caused by the increased emissions of carbon dioxide. In terms of fresh water resources, the annual average river flow will increase as much as 10% - 40% in high latitude and some wet tropical areas and decrease up to 30 % in dry regions at mid-latitude and dry tropical areas (IPCC, 2007). In addition, the IPCC assessment report (2007) warns that flooding will occur much more frequently in coastal areas due to the sea-level rise.

The GCMs have typical spatial resolution between 250 and 600 km, which is too coarse for assessment of regional effects of climatic change. Therefore, downscaling procedures based on large-scale GCM outputs and local information are necessary for the application at regional scales. Different downscaling procedures provide different results for the same GCM output. This means that there is also the uncertainty in the downscaling procedures. In spite of that, the water resources management

researcher is actively dealing with the climate change impacts at local scales (Christensen et al., 2004; Burn, 1998; Simonovic and Li, 2003; Hamlet and Lettenmaier, 1999; Westmacott and Burn, 1997; Payne et al., 2004; Van Rheenen et al., 2004). Most of the published studies focus on the change of weather conditions, such as precipitation, temperature and streamflow. Literature on the application of adaptation measures is very limited. There is a need for development of adaptation strategies for mitigating negative impacts of climate change in practice. They may for example, include reservoir operation rules that will take into consideration a variety of socio-economic impacts of climate change. This study uses an integrated reservoir management system that includes (1) Weather Generator (WG) model; (2) hydrologic model; and (3) optimization model to determine the reservoir operation rules under changing climatic conditions. First, the WG model generates the plausible weather scenarios using observed data and GCM simulation outputs. They are used in the second step as inputs into the hydrologic model. The hydrologic model requires reservoir operating rules and at step three the optimization model selects the optimal set of rules among the alternative choices that optimize the objective function. Therefore, the integrated reservoir management system proposed in this study can be used to determine reservoir operation rules that adapt to new conditions whenever information is available (for example updated GCM output). The results of integrated reservoir management system provide the user with clear indication which part of the basin is vulnerable to climate change and how the reservoir operation should be adjusted to minimize the vulnerability.

1.2 Organization of the report

In the next section, the methodological aspects of K-NN weather generator model, hydrologic model, and optimization model are introduced and the description of their integration is provided. The following section presents the formulation of reservoir optimization model, its objective function and constraints. Study concludes with insights from the integrated reservoir management analyses under climate change and outlines the future work.

2. Methodology

This section of the report provides methodological background of all three key elements of the integrated reservoir management system.

2.1 K-NN Weather Generator (WG) model

The spatial scale of GCMs prevents their effective use in regional assessments of climate change impacts. The downscaling schemes are used to bring the GCM results to regional scales. Dynamic downscaling methods use the GCM results directly as boundary conditions for complex physically -based algorithms that describe atmospheric processes in limited-area models or regional climate models (Jones et al., 1995; Kidson and Thompson, 1998; Wilby et al., 1998). They can generate the regional data equal in length to GCM simulation period. In addition, these methods require significant computational effort and time to provide results on the proper regional scale. Another group of downscaling models is based on statistical downscaling. They have an advantage over dynamic downscaling techniques by using simpler computational procedures (Wilby et al., 2000; Haylock et al., 2006). The process of statistical downscaling is based on the statistical relationships between the GCM output and the observed historical data within a region of interest over the same period. Various tools used for representing these relationships include a linear and nonlinear regression (Wilby et al., 1998), artificial neural networks (Cannon and Whitfield, 2002; Tripathi and Srinivas, 2005), fuzzy rule-based systems (Bardossy et al., 2005), delta method (Smith and Tirpak 1989; Lettenmaier and Gan 1990; Kirshen and Fennessey 1995; Lettenmaier at al. 1999), and quantile mapping method (Wood et al., 2002; Widmann et al., 2003; Salathé, 2004) among others. With the assistance of various downscaling techniques, many researchers have investigated the impact of climate change on water resources at regional scales (Ahmad and Simonovic 2000; Prudhomme et al., 2003; Christensen et al., 2004; Cunderlik and Simonovic, 2004; Simonovic and Li, 2004). The previous studies demonstrate that the climate change induces the change of water

availability (Christensen et al., 2004), extremes (Burn, 1998; Simonovic and Li, 2003), the timing of hydrological events (Hamlet and Lettenmaier, 1999), and the strategies for water resources management (Westmacott and Burn, 1997; Payne et al., 2004; Van Rheenen et al., 2004). Although various downscaling schemes have been used to estimate the impacts of climate change at regional scales, there are still some doubts in the downscaling results because different downscaling techniques employing with exactly the same GCM results provide the different results (Coulibaly and Dibike, 2004).

In some recent work, a Weather Generator (WG) technique is being proposed as another type of statistical downscaling approache. The Weather Generator is regarded as a complex random number generator and has been employed (a) in parametric form as WGEN (Nicks et al., 1990) and generation of weather elements for multiple applications as GEM (Hanson and Johnson, 1998; Parlange and Katz, 2000) or (b) in non-parametric form (Sharma et al., 1997; Wilks and Wilby, 1999; Mehrotra and Sharma, 2007). Parametric weather generators require complex fitting of model parameters. This problem is eliminated the non-parametric methods that are gaining interest among hydrologists. Among non-parametric methods, many successful applications of the K-NN (K-Nearest Neighbor) technique for generating synthetic weather data have been reported (Young, 1994; Lall and Sharma, 1996; Lall et al., 1996; Rajagopalan and Lall, 1999; Buishand and Brandsma, 2001; Yates et al., 2003). Our work builds on the improved K-NN technique of Sharif and Burn (2006).

2.1.1 K-NN Weather Generator (WG) model of Sharif and Burn (2006)

The K-NN algorithm starts with randomly selecting the current day from the observed data set and a specified number of days similar in characteristics to the current day. Using resampling procedure, one of the days from the data set with similar statistical characteristics with current day is selected to represent the weather for the next day. The nearest neighbor algorithm (a) uses a simple computational procedure, and (b) preserves well both, temporal and spatial correlation among the input data. Yates et al. (2003)

applied K-NN algorithm successfully with three variables (precipitation, maximum temperature, and minimum temperature) to diverse areas of United States. The main limitation of their work is that the newly generated data stays within the range of observed minimum and maximum value.

Sharif and Burn (2006) modified the K-NN weather generator algorithm of Yates et al. (2003) by incorporating the perturbation process for weather variables that generates extremes outside the range of historically observed data. The modified K-NN algorithm with p variables and q stations proposed by Sharif and Burn (2006) has the following steps:

1) Calculation of regional means of p variables (x) across all q stations for each day in the historic record:

$$\overline{X_t} = \left[\bar{x}_{1,t}, \bar{x}_{2,t}, \cdots, \bar{x}_{p,t}\right] \qquad \forall\, t = \{1,2,\cdots,T\} \tag{2.1}$$

where
$$\bar{x}_{i,t} = \frac{1}{q}\sum_{j=1}^{q} x_{i,t}^{j} \qquad \forall\, i = \{1,2,\cdots,p\} \tag{2.2}$$

2) Computation of the potential neighbors of size $L = (w + 1) \times N - 1$ days long for each variable p with N years of historical record and selected temporal window of size w. All days within that window are selected as potential neighbors to the current feature vector. Among the potential neighbors, N data corresponding to the current day are eliminated in the process to prevent the possibility of generating the same value as that of the current day.

3) Computation of the regional means for all potential neighbors selected in step 2) across all q stations for each day.

4) Computation of the covariance matrix, C_t, for day t using the data block of size $L \times p$.

5) Random selection of the first time step value for each variable p from all current day values in the record of N years.

6) Computation of the Mahalanobis distance expressed by Eq. (2.3) between the mean vector of the current days ($\overline{X}_t$) and the mean vector of all nearest neighbor values ($\overline{X}_k$), where $k = 1, 2, \cdots, L$.

$$d_k = \sqrt{\left(\overline{X}_t - \overline{X}_k\right) C_t^{-1} \left(\overline{X}_t - \overline{X}_k\right)^{\mathrm{T}}} \tag{2.3}$$

where T represents the transpose matrix operation, and C^{-1} represents inverse of covariance matrix.

7) Selection of the number of $K = \sqrt{L}$ nearest neighbors out of L potential values.

8) Sorting the Mahalanobis distance d_k from smallest to largest, and retaining the first K neighbors in the sorted list (they are referred to as the K Nearest Neighbors). Then, use a discrete probability distribution giving higher weights to closest neighbors for resampling out the set of K neighbors (Lall and Sharma, 1996). The weights are calculated for each k neighbor using the following Eq. (2.4) and (2.5).

$$w_k = \frac{1/k}{\sum_{i=1}^{K} 1/i} \tag{2.4}$$

where $k = 1, 2, \ldots, K$. Cumulative probabilities, p_j, are given by:

$$p_j = \sum_{i=1}^{j} w_i \tag{2.5}$$

Note that Sharif and Burn (2006) used cumulative probability of K neighbors with Eq. (2.5) while Yates et al. (2003) used just a probability for each K neighbors as shown by Eq. (2.4).

9) Generating random number $u(0,1)$ and comparing it to the cumulative probability p_j to determine the nearest neighbor of current day. If $p_1 < u < p_K$, then day j for which u is closest to p_j is selected. On the other hand, if $u < p_1$, then the day corresponding to d_1 is selected, and if $u = p_K$, then the day corresponding to d_K is selected. Once the nearest neighbor is selected, the weather of selected day is used for all stations in the region. This is how the K-NN algorithm preserves the cross-correlation among variables in the region. In this step, the improved K-NN algorithm offers a reasonable method that randomly selects one among K neighbors based on the cumulative probability. However in the algorithm by Yates et al. (2003) the first nearest neighbor may be

selected in most cases because it selects one of K nearest neighbors for which u is closest to a probability of each neighbor.

10) This step is added by Sharif and Burn (2006) to generate variables outside the range of historical data by perturbation. First, estimation of a conditional standard deviation σ for K nearest neighbors, and bandwidth λ (Sharma et al., 1997) is performed using Eq. (2.6):

$$\lambda = 1.06\,\sigma\,K^{1/5} \tag{2.6}$$

Then, the perturbation process follows according to Eq. (7):

$$y_{i,t}^{j} = x_{i,t}^{j} + \lambda \sigma_i^j z_t \tag{2.7}$$

where $x_{i,t}^{j}$ is the value of the weather variable obtained from the original K-NN algorithm; $y_{i,t}^{j}$ is the weather variable value from the perturbed set; z_t is normally distributed random variable with zero mean and unit variance, for day t. To prevent the negative values for bounded variables (i.e. precipitation), the largest acceptable value of $\lambda_a = x_{*,t}^{j} / 1.55\sigma_*^j$ is employed, where * refers to a bounded weather variable (Sharif and Burn, 2006). If the value of the bounded weather variable, computed previously, is still negative, then a new value of z_t is generated.

2.1.2 Integration of weather generator with principle component analysis (WG-PCA)

Sharif and Burn (2006) have developed the weather generator coded in C^{++} language employing the improved K-NN algorithm with three variables (p = 3: precipitation, maximum temperature, and minimum temperature). They generated 800 years of weather data with improved K-NN algorithm for the Upper Thames River basin, Ontario, Canada and showed that the modified algorithm generates synthetic data maintaining the statistical characteristics of reference data. The main conclusion of their work is that the modified K-NN algorithm has the potential to serves as a tool for generating plausible scenarios for

the effective water resources management. However, one drawback of their work still remains – the modified algorithm cannot reflect the leap year (only generates weather data for 28 days in February).

Prodanovic and Simonovic (2006a, 2006b) revised the weather generator developed by Sharif and Burn (2006) to address the leap year deficiency in the model and analyze the climatic change impacts on high flows (Prodanovic and Simonovic, 2006a) and low flows (Prodanovic and Simonovic, 2006b). The algorithm is converted into JAVA programming language and used in conjunction with a rainfall-runoff model (HEC-HMS) for the Upper Thames River basin, Ontario, Canada. Since the HEC-HMS model requires only the precipitation as a meteorological input they have employed only the precipitation data (p = 1) in the weather generator model to simplify its application. Both WG models developed in previous studies can generate the precipitation very well. However, the model employing more variables has the potential to capture the characteristics of the current weather with more detail because larger number of variables (i.e. temperature, humidity, pressure, etc.) provides additional information for choosing the nearest neighbor.

This study (a) revised the WG model to allow the use of more variables available in the basin and (b) investigated the sensitivity of the results to the choice of variables. If there are many meteorological variables available in the basin for use with the WG model, the calculation of Mahalanobis distance expressed by Eq. (2.3) becomes quite demanding. Therefore, in this study we proposed integration of WG model with the Principle Component Analysis (PCA). The new model named WG-PCA, reduces the dimension of the mean vector of the current days ($\overline{X}_t$) and the mean vector of all nearest neighbor values ($\overline{X}_k$) in Step (6). The new approach requires only the variance of the first principle component to calculate the Mahalanobis distance. The WG-PCA modifies the Step (6) of the algorithm presented in the previous section as follows:

(a) Calculation of eigenvector and eigenvalue for the covariance matrix (C_l).

(b) Finding the eigenvector related to the largest eigenvalue that explains the largest fraction of the variance described by the p variables.

(c) Calculation of the first principle component with the eigenvector found in step (b) using Eq. (2.8) and Eq. (2.9):

$$PC_t = \overline{\mathbf{X}}_t \mathbf{E} \tag{2.8}$$

$$PC_k = \overline{\mathbf{X}}_k \mathbf{E} \tag{2.9}$$

where PC_t and PC_k are the values of current day and the nearest neighbor transferred by the eigenvector found in step (b), respectively; and **E** is the eigenvector related to the largest eigenvalue.

After calculating the PC_t and PC_k with one-dimensional matrix obtained by Eq (2.8) and (2.9), the Mahalanobis distance is computed using Eq. (2.10):

$$d_k = \sqrt{\left(PC_t - PC_k\right)^2 / \mathrm{Var}(\mathbf{PC})} \quad \forall k = \{1,2,\cdots,K\} \tag{2.10}$$

where Var(**PC**) represents the variance of the first principle component for the K nearest neighbors.

In summary, this study used three WG models: (a) Sharif and Burn (2006) WG with one variable (precipitation) named WG1, (b) Sharif and Burn (2006) WG with three variables named WG3, and (c) WG combined with PCA using three variables named WG-PCA3. Results obtained using three different models are compared with each other to investigate the effects of additional variables in K-NN algorithm. In addition, the comparison of original WG model with WG-PCA is performed too.

2.2 Hydrologic model (HEC-HMS)

Various weather conditions obtained using weather generators are further used as inputs into hydrologic models in order to further assess the impacts of climate change on local conditions in a basin.

Hydrologic models are mathematical representations of rainfall-runoff processes operating within a basin. They provide essential information for the management of storage facilities-reservoirs in the basin. Therefore, hydrologic model is one important component of the integrated reservoir management system developed in this research as a tool for the analyses of climate change adaptation options within a basin.

The hydrologic model employed in this study is based on the United States Army Corps of Engineers, Hydrologic Engineering Center's Hydrologic Modeling System (HEC-HMS) which consists of three modules: (i) meteorologic module which describes basin input processes such as precipitation, evapotranspiration and other; (ii) basin module which describes the main physical processes occurring within a basin; and (iii) control module that sets the simulation parameters. The meteorologic and basin modules consist of a collection of methods allowing the user to specify and describe climatic and physical properties of the basin.

HEC – HMS hydrologic model can be used as event-driven or continuous-process model (Cunderlik and Simonovic, 2004 and 2005). Event-driven models are designed to simulate individual precipitation-runoff events. Their emphasis is placed on infiltration and surface runoff, their objective is the evaluation of direct runoff. Typically, event models have no provision for moisture recovery between storm events and, therefore, are not suited for the simulation of dry weather flows (drought analyses). Continuous-process models on the other hand take explicit account of all runoff components, including direct and indirect runoff (Bennett, 1998). They focus on long-term hydrologic abstractions responsible for the rate of moisture recovery during the periods of no precipitation. They are suited for simulation of daily, monthly or seasonal streamflow, usually for long-term runoff-volume forecasting and for estimates of water yield.

The integrated reservoir management system uses the HEC – HMS hydrologic model in continuous form that provides a detailed long term movement of moisture within the basin, as well as an elaborate representation of moisture losses. Continuous hydrologic models (Fig. 2.1) typically combine methods used to describe rainfall transformation, baseflow, channel/reservoir routing (determining the shape of a

flood hydrograph as it moves through a channel/reservoir), together with losses (detailed movement of water through vegetation, surface, soil and ground water).

Cunderlik and Simonovic (2004) have developed the event and continuous hydrological models for the Upper Thames River basin and Prodanovic and Simonovic (2006a, 2006b) applied these models within an inverse approach for assessment of the flood and drought risk under climate change. However, the previous work did not address the problem of optimal reservoir operation. The releases from the reservoirs in the basin were decided using the simple relationship between storage and outflow. In this study we modified the reservoir module to introduce a rule curve for control of reservoirs. The overall structure of the modified continuous hydrologic model is shown in Fig. 2.2, where each box represents a module that mathematically describes a physical process in the basin. The snow module adjusts precipitation to account for both solid and liquid precipitation using the input (precipitation and temperature) from the weather generator. The output of the snow module is used for computation of losses. The losses module describes the movement of moisture through various conceptual reservoirs within a catchment, which provides four different types of outputs; (1) evapotranspiration, or moisture that evaporates from the canopy, surface depressions, and/or the soil, (2) baseflow, (3) surface excess that does not infiltrate into the soil, and (4) ground water recharge that enters into deep aquifers and does not return to the stream. The surface excess is used by the transform module to generate surface runoff, which is then combined with baseflow to produce direct runoff. Then, the direct runoff is used by the routing module to calculate the propagation of a flood wave eventually producing channel streamflow. The reservoir module, employing the reservoir rule curve, is run if a reservoir exists at the end of a channel.

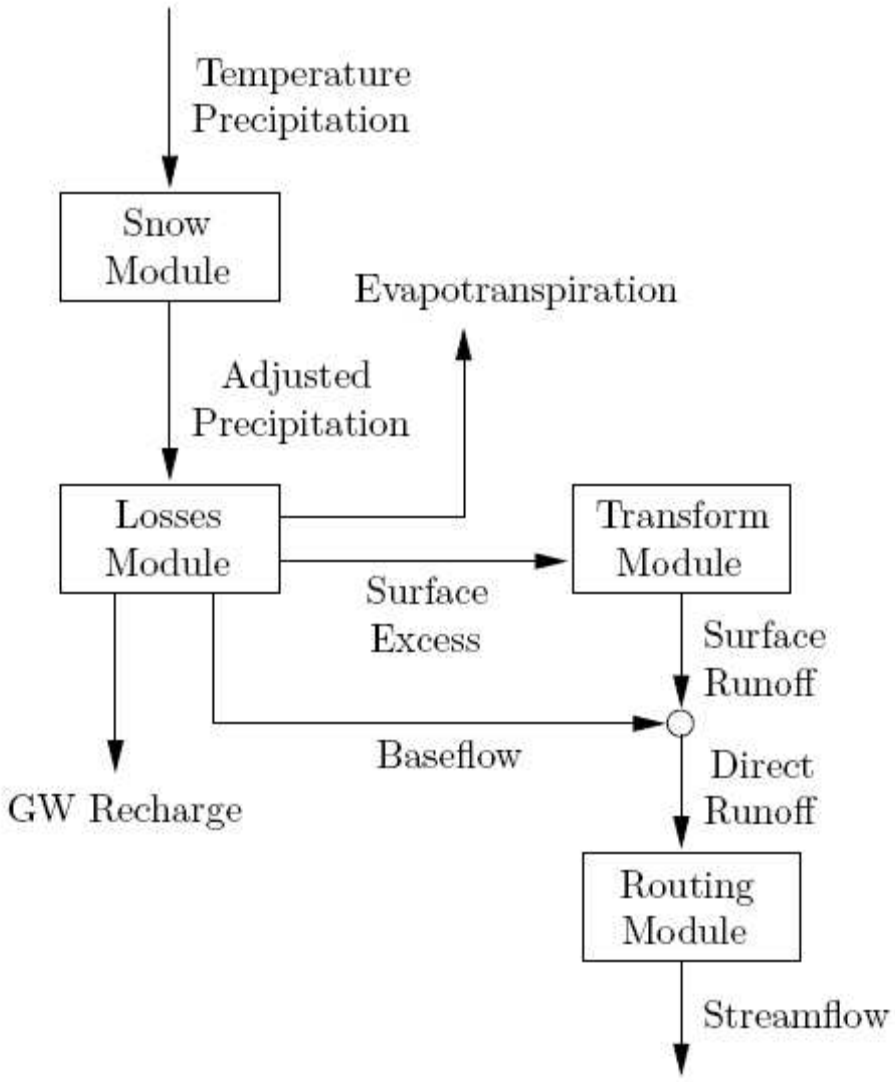

Figure 2.1 Continuous hydrologic model structure

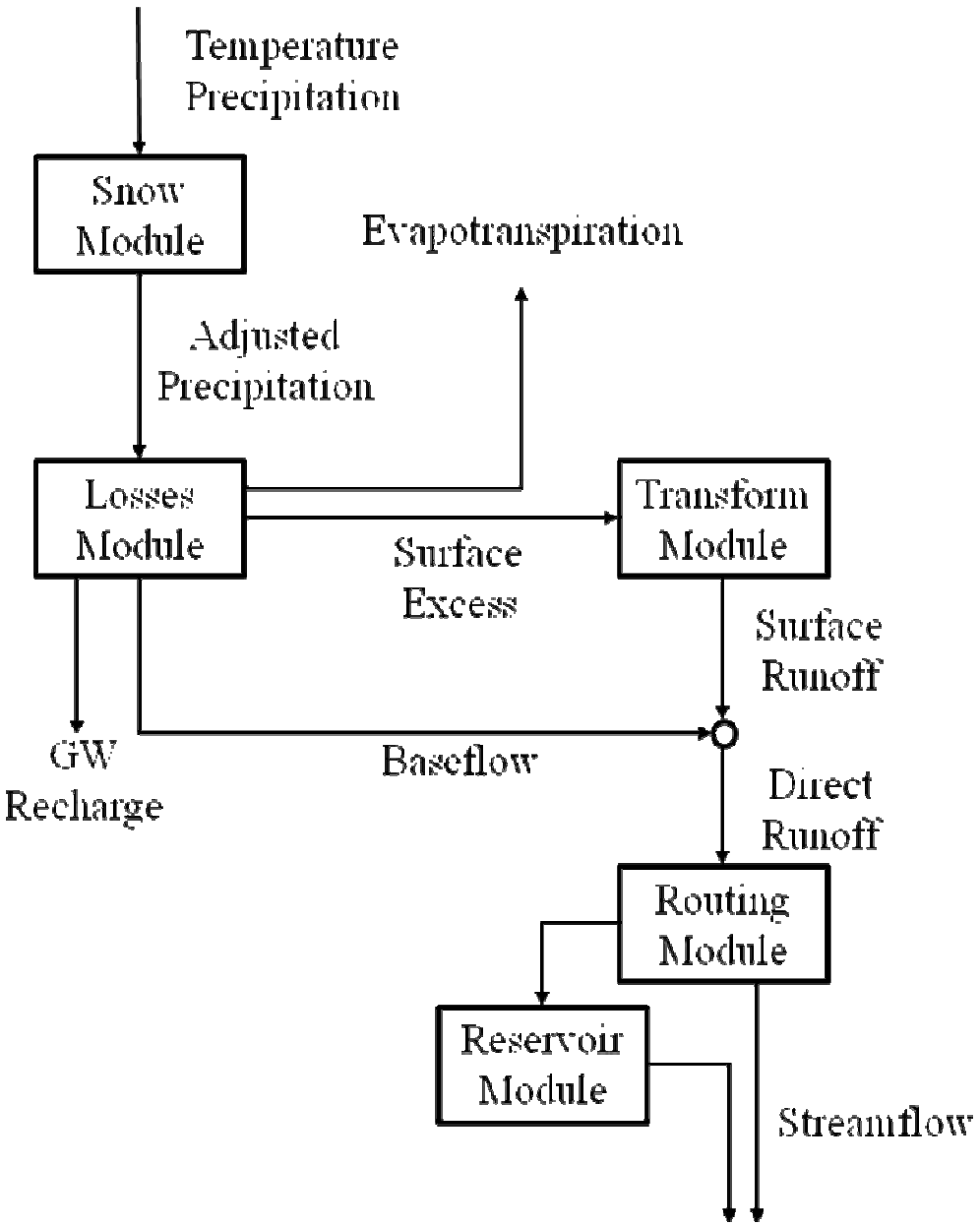

Figure 2.2 Modified continuous hydrologic model structure

2.3 Optimization model

Many optimization schemes have been employed to provide the efficient solutions to reservoir management problems (Yeh, 1985; Labadie, 2004). Nowadays, there are many nonlinear optimization algorithms that work using gradient-based and heuristic-based search techniques in deterministic and stochastic contexts. Traditional optimization approaches are showing some limitations for application with more complex reservoir management problems. Therefore, algorithms based on natural and physical selection principles are being adopted for more robust optimization. To mimic the natural selection phenomenon or physical selection principles, several algorithms under the general umbrella of evolutionary optimization are suggested. They include genetic algorithms (Holland, 1975; Goldberg, 1989), simulated annealing (Kirkpatrick et al., 1983), ant colony optimization (Dorigo, 1992), memetic algorithms (Moscato, 1989), and particle swarm optimization (Eberhart and Kennedy, 1995). Over the last decade, evolutionary optimization algorithms have been extensively used in various problem domains and succeeded in effectively finding the near global optimal solutions.

Differential Evolution (DE) algorithm is used in this study. It has been introduced by Price and Storn (1997) as a branch of evolutionary algorithms for optimization problems over continuous domains. DE has been applied to various science and engineering fields. Its main advantages include simple structure, ease of use, fast convergence, and robustness. If a system can be evaluated rationally, DE can provide the effective means to select the best possible solution. DE uses mutation as a search mechanism and selection to direct the search toward the prospective regions in the feasible region. Therefore, DE uses *mutation* as the primary search mechanism while Genetic Algorithm (GA) uses *crossover*, a mechanism of probabilistic exchange of information among solutions to locate better solutions.

DE is a population based search technique which utilizes NP variables as population of D dimensional parameter vectors for each generation. The initial population is chosen randomly in most cases. In the case of available preliminary solution, the initial population can be generated by adding

normally distributed random values to the preliminary solution. The basic idea behind DE is to generate trial parameter vectors by adding the weighted difference vector between two population members to a third member described by Eq. (2.11) and crossover process.

$$X_c^{'} = X_c + F(X_a - X_b) \tag{2.11}$$

where $X_c^{'}$ represents a vector before crossover, X_a, X_b, and X_c are vectors chosen randomly to define a vector differential and trial vector, and F is the weighting or scaling factor given by user in the optimal range between 0.5 and 1.0 (DE, 2008). Therefore, the trial vector is the child of two parents, a noisy random vector and the target vector against which it must compete. Uniform crossover that takes vector parameters from one parent more often than it does from other is used with a crossover constant (CR), in the optimal range between 0.5 and 1.0, which represents the probability that the child vector inherits the parameter values from the noisy random vector (DE, 2008). For example, when CR = 1.0, every trial vector parameter is certain to come from $X_c^{'}$. On the other hand, when CR = 0, all but one trial vector parameter comes from the target vector. When CR = 0, the final trial vector parameter must come from the noisy random vector to ensure that X_t differs from X_i by at least one parameter. Finally, the objective function corresponding to the trial vector is compared with that of the target vector. Then, the vector resulting in the lower objective function value in minimization problem among two vectors would survive for the next generation. Graphical representation of the DE optimization process is shown in Fig. 2.3. The search process continues until the termination criterion of a preset maximum iteration number is met, and difference in objective function values between two consecutive generations satisfies the tolerance level given by user.

After Price and Storn (1997) have given first the working principle of DE with single strategy, they suggested nine more strategies that vary based on the vector to be perturbed, number of difference vectors, and the type of crossover (Onwubolu and Babu, 2004; Price et al., 2005). Different strategies can be

adopted in the DE algorithm depending upon the type of problem to which DE is applied. A strategy that works out to be the best for a certain problem may not work well for a different problem. Therefore, the strategy and the key parameters to be used for a particular problem should be determined by trial and error. However, strategy employing random perturbation, one difference vector, and binomial crossover scheme to generate a trial vector appears to be the most successful and the most widely used strategy.

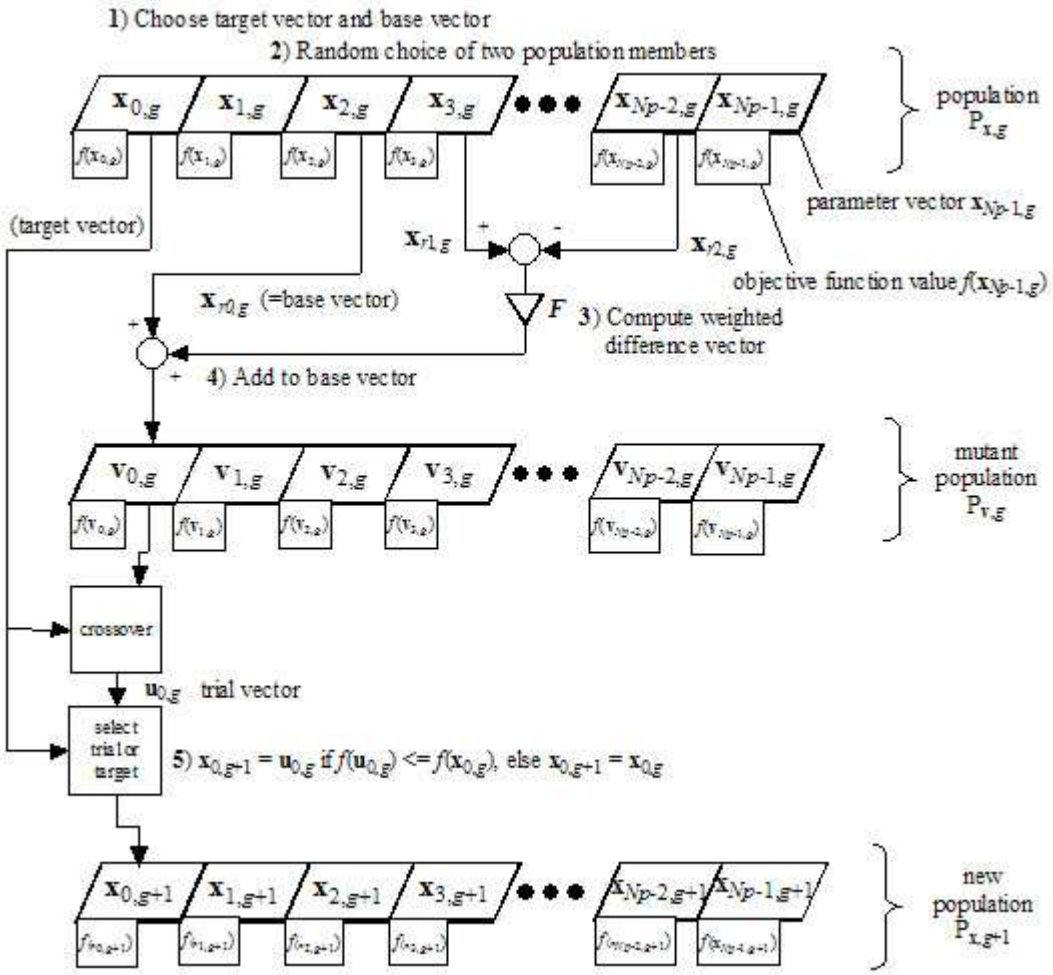

Figure 2.3 Differential evolution algorithm

(http://www.icsi.berkeley.edu/~storn/code.html#hist)

3. Integrated Reservoir Management System

In this study three separately developed models are integrated into a reservoir management system: 1) WG model for downscaling the GCM output, 2) modified hydrological model for generating the streamflow in the basin, and 3) DE optimization model for determining the optimal reservoir adaptation to changing climatic conditions.

The procedure for finding the optimal solution is shown in Fig. 3.1. It is divided into 3 steps. First, the weather generator model generates weather conditions based on the available GCM outputs. This process can be easily repeated for any new and/or improved GCM output. Second, the output of weather generator model is put into the modified continuous hydrologic simulation model to estimate the basin response. This model allows for determination of damages and/or benefits corresponding to the optimal reservoir adaptation response to future climate scenarios. The reservoir adaptation is provided by the optimization module. Therefore, the hydrologic model plays a key role in the integrated system. It receives both, the weather conditions and reservoir adaptation strategies from weather generator module and optimization module, respectively. In addition, it provides the response of the basin to easily understand the impacts of different climate scenarios on each control point within the basin. Lastly, the optimization model generates the optimal reservoir operations rule curves as adaptation strategy to changing climatic conditions in the basin. The integrated reservoir management model results interpretation procedure is shown in Fig. 3.2. It offers the statistical analyses and provides valuable guidelines for reservoir adaptation to changing climate conditions.

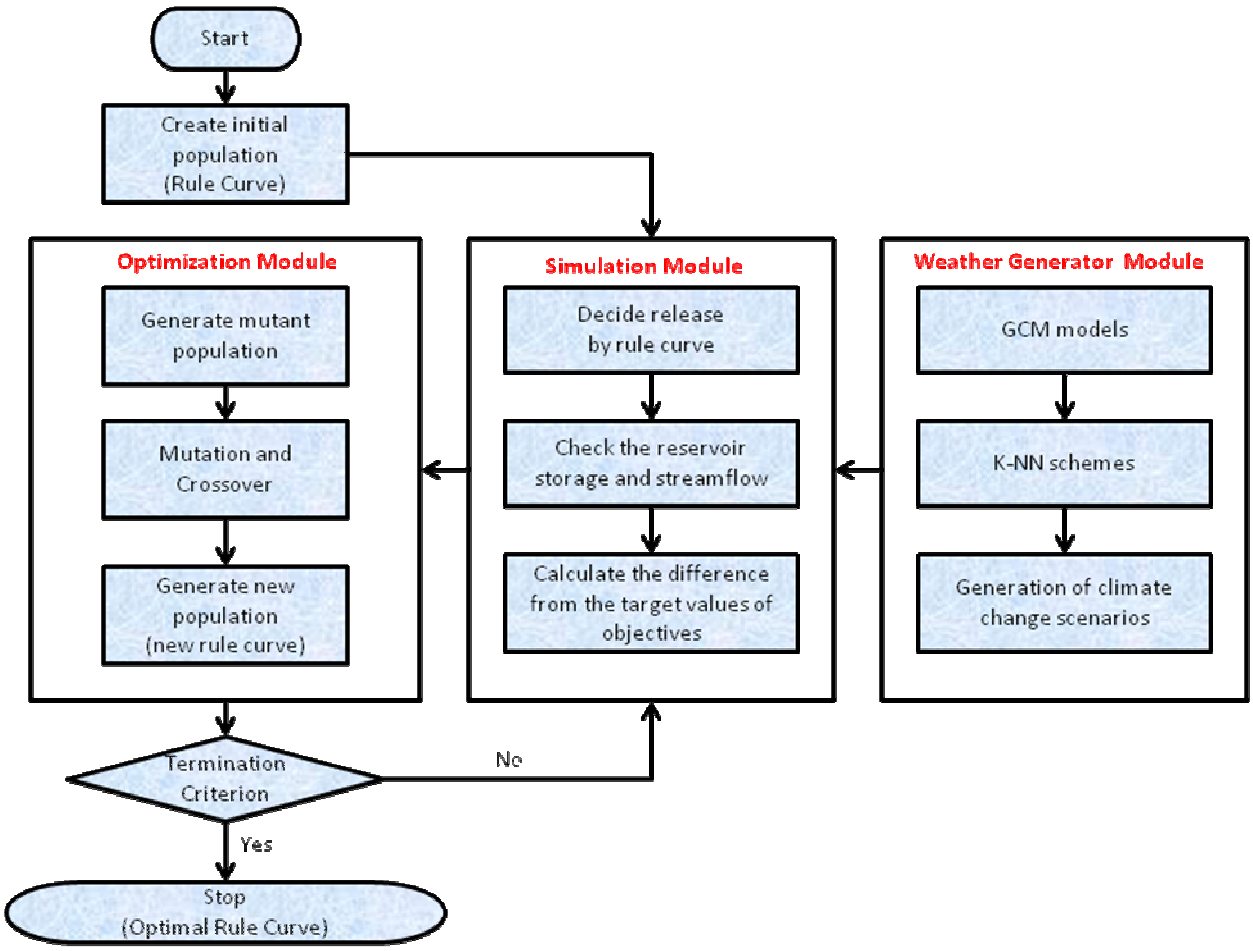

Figure 3.1 Optimization procedure of the integrated reservoir management system

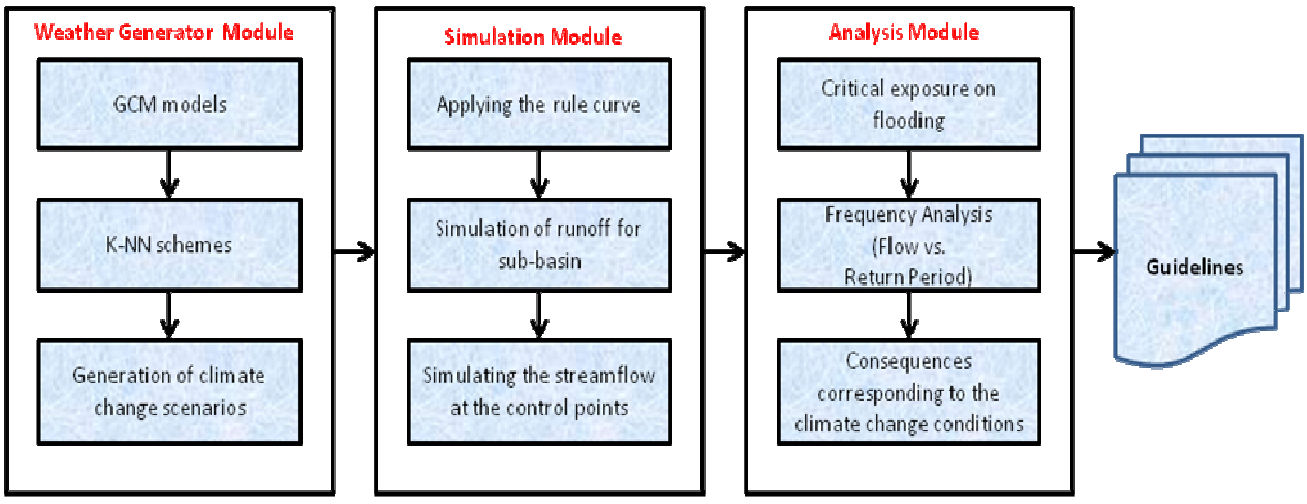

Figure 3.2 Interpretation procedure of integrated reservoir management system

4. Application

4.1 Study basin – The Upper Thames River basin

The Thames River basin consisting of two major tributaries has a drainage area of 3,482 km^2. The stream length is 273 km (from Tavistock to its mouth at Lake St. Clair): the North Branch, flowing southward through Mitchell, St. Marys, and eventually into London, and the East Branch, flowing through Woodstock, Ingersoll, and east London (Fig. 4.1). The two branches join near London city and then the river flows westwards and exits the basin near Byron, eventually draining into Lake St. Clair. The Upper Thames River basin receives about 1,000 mm of annual precipitation, 60% of which is lost through evaporation and/or evapotranspiration, stored in ponds and wetlands, or recharged as ground water (Wilcox et al., 1998). The slope is about 1.9 m/km for most of its upper reaches, while its lower reaches are much flatter with a slope of less than 0.2 m/km.

The Upper Thames River basin has three major water management reservoirs: Wildwood, Pittock and Fanshawe near St. Marys, Woodstock and London, respectively (Fig. 4.1). The primary goals of all reservoirs include the flood control during snowmelt period and summer storm season, low flow augmentation from May to October, and recreational uses during the summer season. Among these goals, the most important goal is flood control. Floods in the basin result from a combination of snowmelt and intensive precipitation during December to April. The basin has the facilities like extensive dyking systems and a diversion channel to prevent the flood damages. Summer frontal storms are also known to produce severe flooding in and around the basin, but such storms are less frequent. Drought conditions occur mostly from June to September, though they can occur at any time of the year (Cunderlik and Simonovic, 2004).

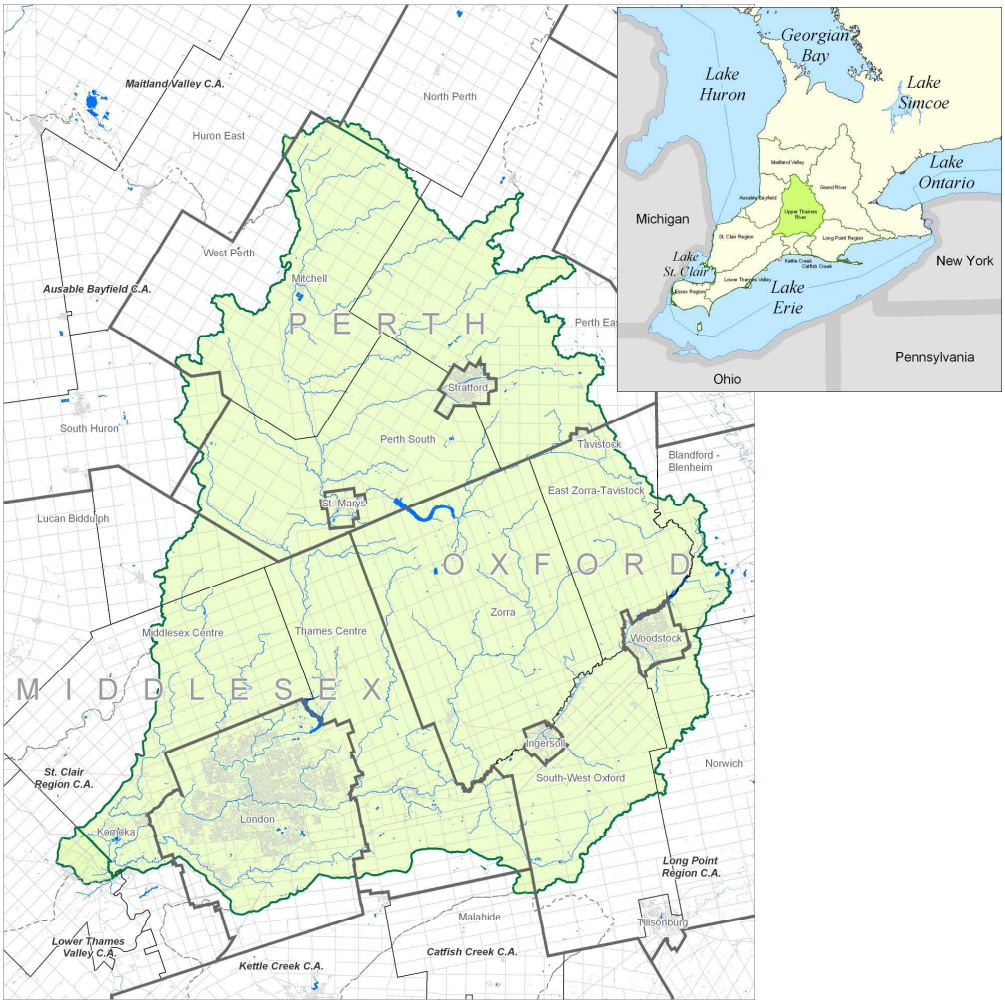

Figure 4.1 Schematic map of the Upper Thames River basin

4.2 Application of K-NN Weather Generator model

This study uses daily precipitation, maximum temperature, and minimum temperature of 15 stations for the period from 1964 to 2001 ($N = 38$) to simulate the plausible meteorological scenarios. Employing the temporal window of 14 days ($w = 14$) and 38 years of historical data ($N = 38$), this study used 569 days as the potential neighbors ($L = (w + 1) \times N - 1 = 569$) for each variable. The schematic location map and meteorological characteristics of 15 stations in the basin are shown in Fig. 4.2 and Fig. 4.3.

Only three locations are used to show the comparison of WG results (data for other locations are available upon request): (1) Stratford for illustrating the characteristic of the northern part of the basin, (2) London for south-western part, and (3) Woodstock for south-eastern part of the basin. The monthly characteristics of the variables considered in this study are shown in Fig. 4.4. The results for three stations, therefore, will be represented and compared later for three WG models introduced in Section 2.1 of this report.

This study generated synthetic meteorological scenarios equal in length to the historical data to allow for the statistical comparison of synthetic and historical data. Note that in the case of WG1 model, all variables recorded in the basin can be generated (all records on the day selected by K-NN algorithm are available) even though Mahalanobis distance is calculated based on one variable only (precipitation) to select the nearest neighbors. Therefore, all models used in the study generate three variables available in the Upper Thames River basin. That allows for comparison of different weather generator models with each other.

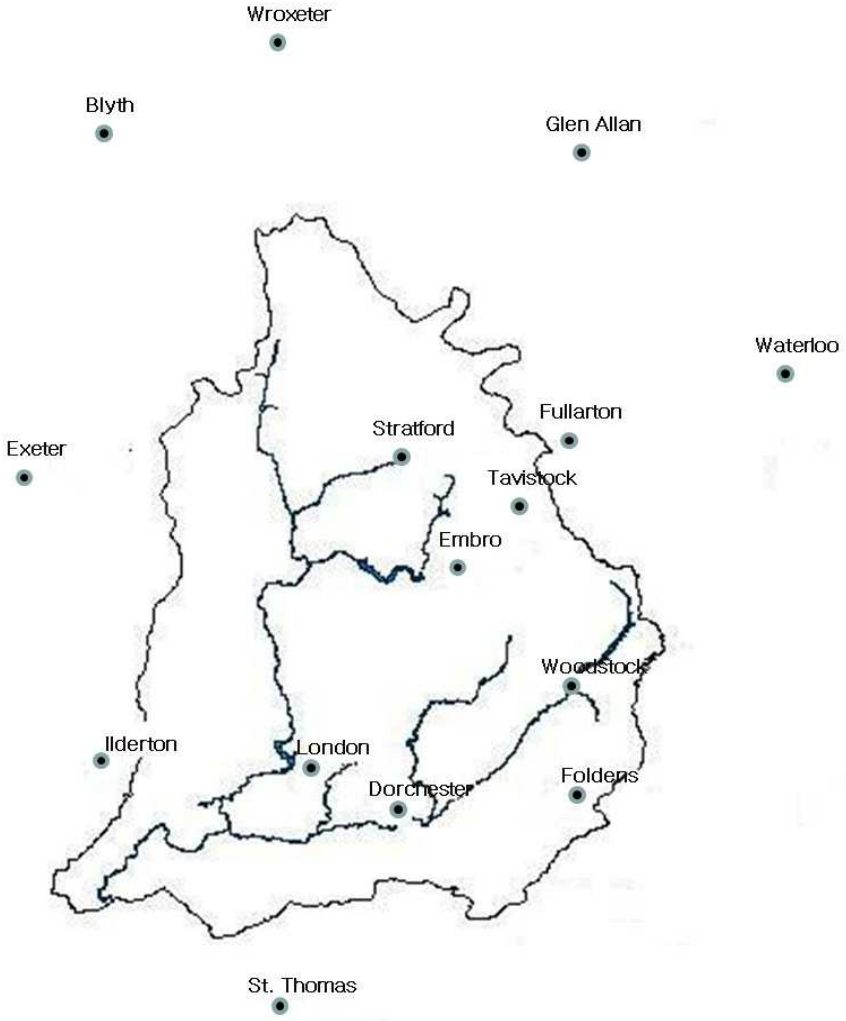

Figure 4.2 Schematic location map of stations in the basin

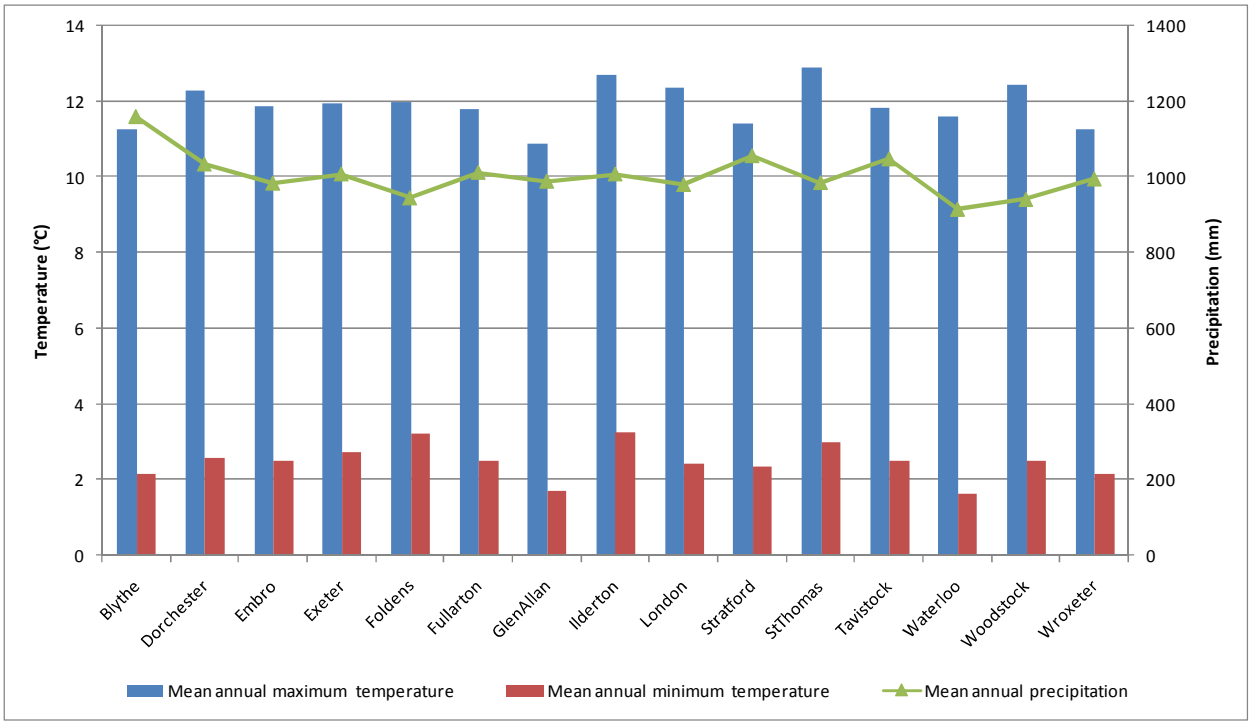

Figure 4.3 Meteorological characteristics of stations in the basin

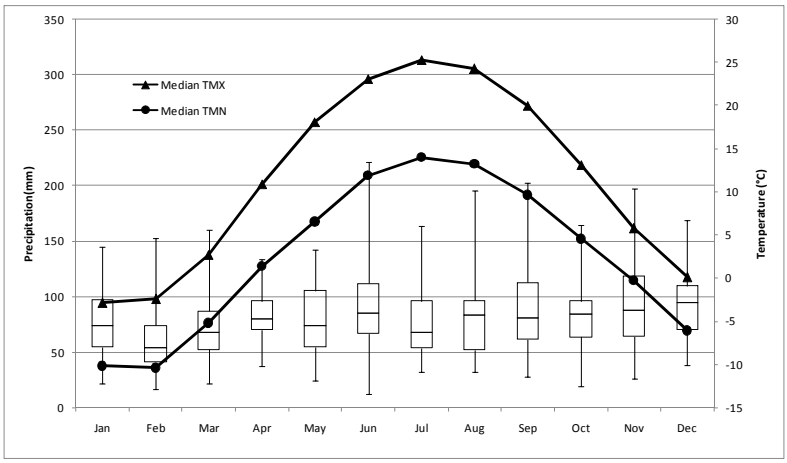

(a) Stratford

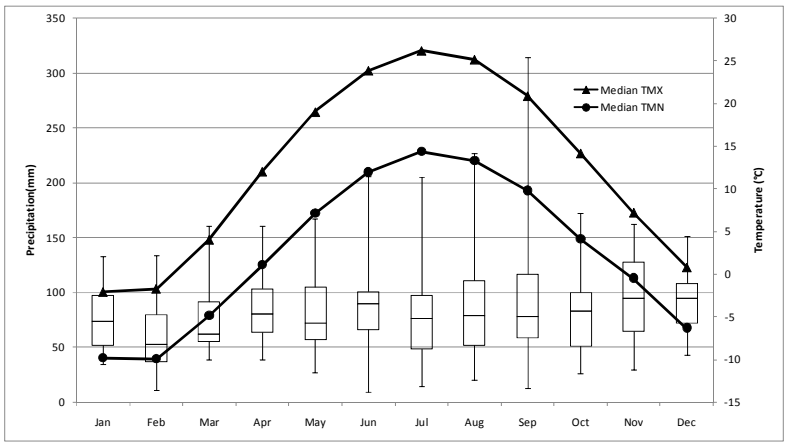

(b) London

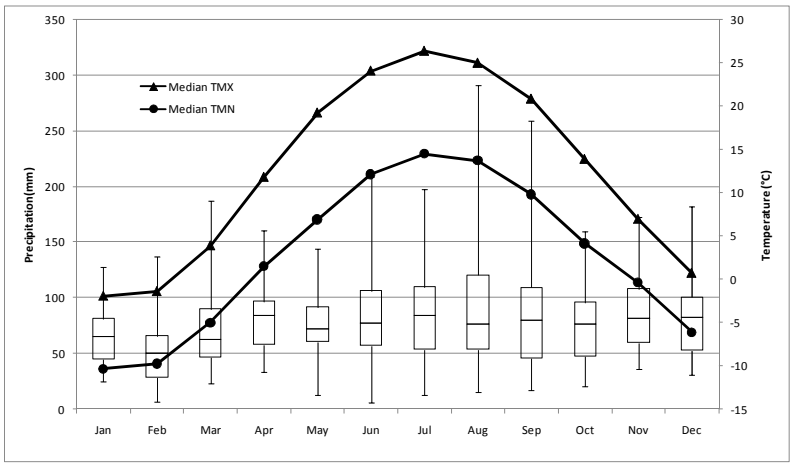

(c) Woodstock

Figure 4.4 Statistical characteristics of three representative stations

4.3 Application of the hydrologic model

Cunderlik and Simonovic (2004a, 2005) have developed the continuous hydrologic model for the Upper Thames River basin. The model has been properly calibrated and verified, with extensive sensitivity analyses. The continuous hydrologic model consists of 34 sub-basins, twenty one river reaches, and three reservoirs. The schematic of the continuous model is shown in Fig. 4.5. The model uses a different parameter sets for describing summer and winter seasons. The model details are provided in Cunderlik and Simonovic (2004a, 2004b, 2005) and in Prodanovic and Simonovic (2007).

The previous studies conducted with the model have applied the channel routing method, referred to as the Modified Plus method, to reservoirs, with a non-linear relationship between the storage and outflow based generally on the historical reservoir operations data. However, this relationship between the storage and outflow changes with changing weather conditions (caused by climate change). In addition, the optimal reservoir operations are needed as an adaptation strategy for accommodating monthly or seasonal hydrological conditions caused by climate change. This study developed an integrated reservoir management model for optimization of monthly reservoir operational rule curves as introduced in the Section 3 of the report. To estimate the flood damages caused by summer storm or snow melting during a short time periods (1 day or 2 days) at different control points in the basin, hourly or daily reservoir rule curves are required. In case of hourly rule curve, reservoir optimization model requires 8,760 (=365×24) decision variables within one year. A large number of decision variables extends the optimization computation time. Therefore, this study incorporated an interpolation scheme into the reservoir optimization model which uses a monthly rule curve in to an hourly-based reservoir operations simulation. The hydrological model has a time-step limitation because Clark's time of concentration is 6 hours (used as the minimum time-step) within some sub-basins. This study employs 6 hours time-step to simulate the streamflow and to estimate the corresponding climate change impacts based on the optimal rule curves and various climate scenarios.

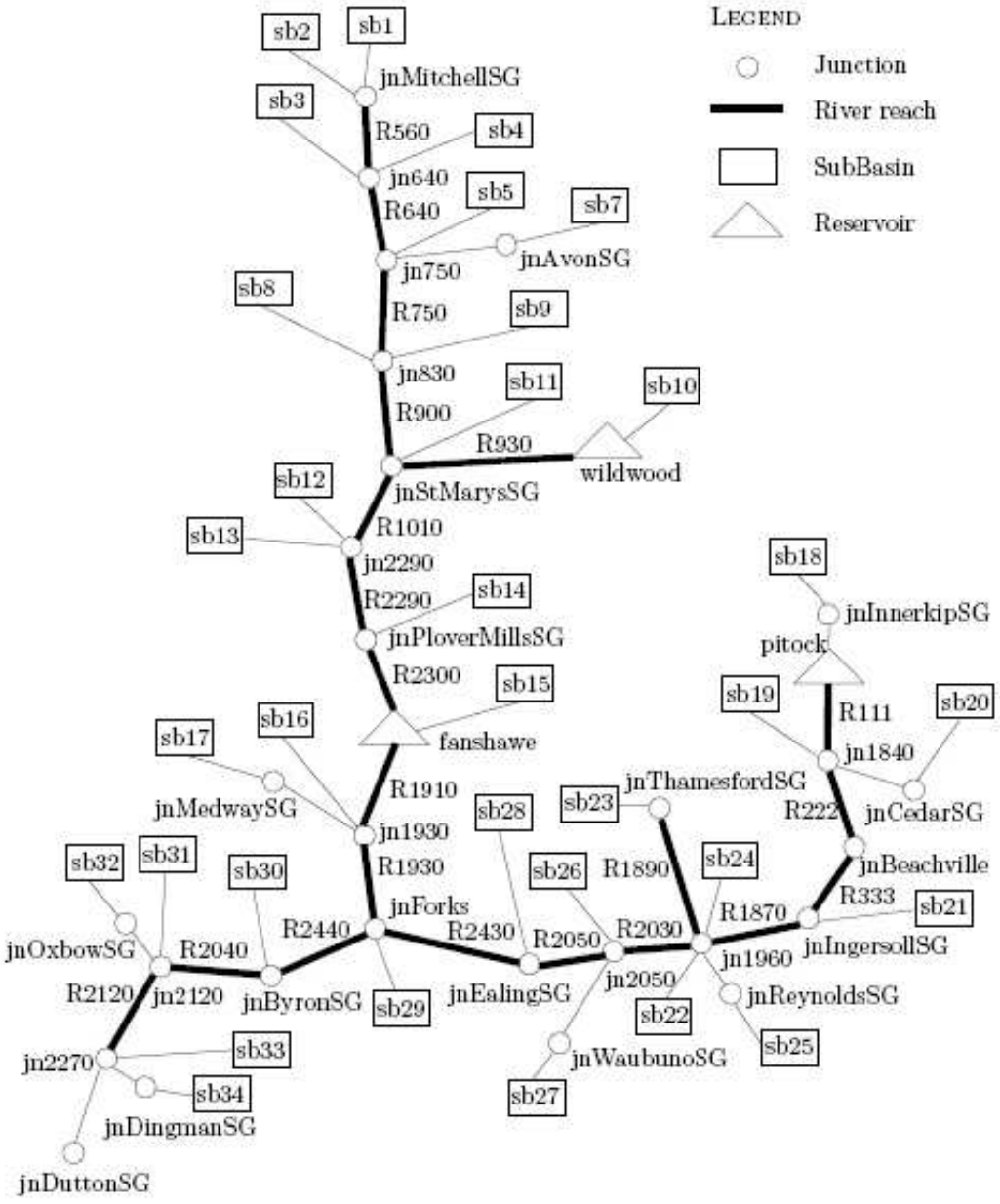

Figure 4.5 Schematic of the hydrologic model for the Upper Thames River basin

4.4 Optimization model (Differential Evolution, DE)

4.4.1 Objective function

Optimization can be defined as a process that searches for an optimal solution that provides a maximum or minimum value of an objective function (Rao, 1996). Therefore, formulation of the objective function is the most important step in solving an optimization problem.

The objective function used in this study is formulated as shown in Eq. (4.1).

$$\min f = \sum w_i D_i \tag{4.1}$$

where D_i represents the flood damage at control point i and w_i is the weighting factor assigned corresponding to the importance of control points.

The Upper Thames River Conservation Authority (UTRCA) suggested the consideration of the following flood damage points in the basin: Mitchell, StMarys, Byron, Ingersoll, and Ealing (UTRCA, 2005). In addition, flood damage tables (as function of streamflow value) have been developed for each damage point. In this study four control points are selected and used in the formulation of the objective function as shown in Table. 4.1. In addition, the weighting factors should be assigned according to the importance of each control point. Available flood damage tables are used to extract the importance of each control point proportional to the level of total flood damage as shown in Eq. (4.2).

$$w_i = \frac{\text{Maximum } Di}{\sum_j \text{Maximum } D_j} \tag{4.2}$$

For example, the maximum flood damages at Byron, Ingersoll, and StMarys are $ 32,314,800., $ 22,246,300., and $ 13,627,400., respectively. The resulting weighting factors for Byron, Ingersoll, and StMarys are then 0.47, 0.33, and 0.20, respectively. Use of the flood damage tables in the determination of weighting factors has an advantage that their values can be easily modified if/when updated flood damage tables become available. Using the flood damage tables provided by UTRCA (2005) for four control points as shown in Figure 4.6, this study determined the weighting factors of 0.35, 0.26, 0.24 and 0.15 for Byron, Ealing, Ingersoll and StMarys, respectively.

Table 4.1 Available damage points in the Upper Thames River basin

Available damage points	Points not affected by the reservoirs	Usable points for development of the reservoir operations rule curve
Mitchell, StMarys, Medway	Mitchell	StMarys, Byron
Byron, Ingersoll, Ealing	Medway	Ingersoll, Ealing

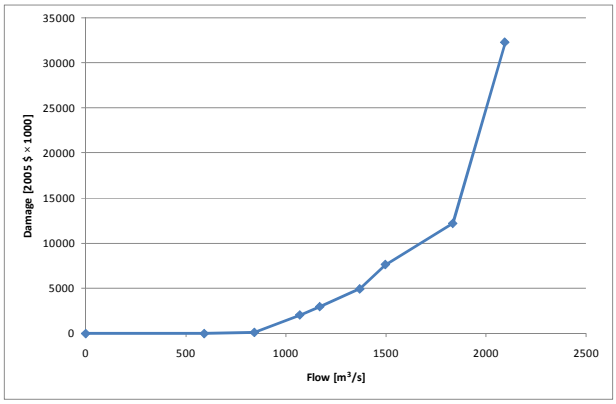

(a) Byron

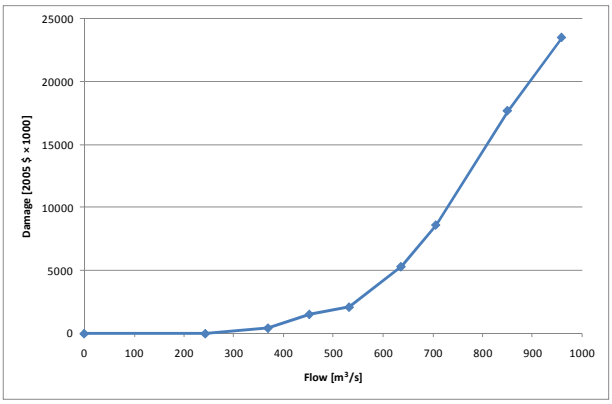

(b) Ealing

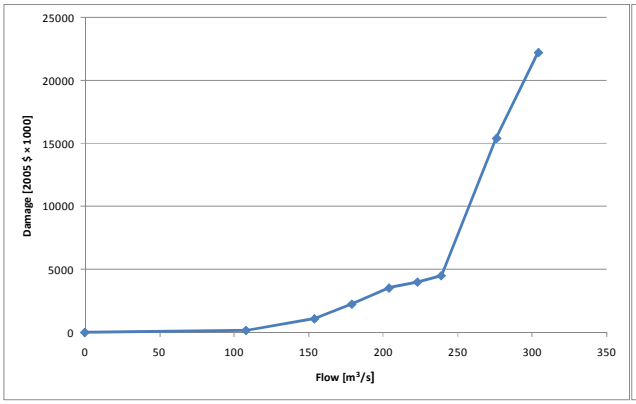

(c) Ingersoll

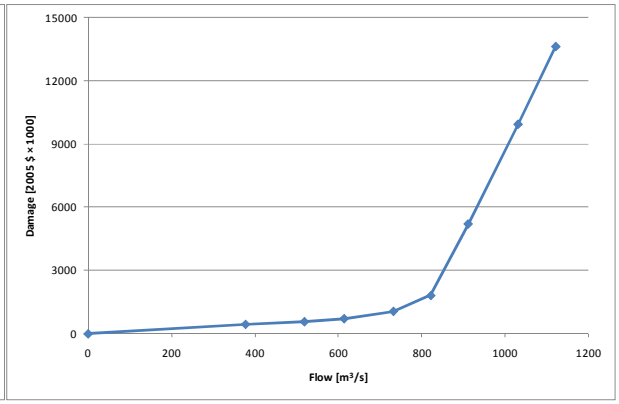

(d) StMarys

Figure 4.6 Flood damage curves for four control points in the Upper Thames River basin

4.4.2 Constraints on reservoir operations

The Upper Thames River basin consists of three reservoirs - Fanshawe, Wildwood, and Pittock. The physical constraints for all reservoirs are provided in Table 4.2. The UTRCA in 1993 conducted a study(UTRCA, 1993) to develop the rule curves for Wildwood and Pittock reservoirs for satisfying the seasonal needs of water supply and flood control. The operational constraints taken from the 1993 study for two reservoirs are shown in Table 4.3.

The optimization problem addressed in this work determines the optimal set of rule curves for all reservoirs. The two types of monthly rule curves are developed: (1) lower rule curves and 2) upper rule curve. With 12 months optimization horizon the optimization algorithm determined the release according to four cases presented in Eq. (4.4) to Eq. (4.7) and the continuity Eq. (4.3).

$$S_t^i = S_{t-1}^i + I_t^i - R_{t,i}^{\text{req}} \tag{4.3}$$

Case 1: Reservoir storage below the lower rule curve

$$R_t^{\text{i}} = R_{t,i}^{\text{req}} \left(S_t^{\text{i}} - S_i^{\min} \right) / \left(S_{t,i}^{\text{lower}} - S_i^{\min} \right) \tag{4.4}$$

Case 2: Reservoir storage between the lower and the upper rule curve

$$R_t^{\text{i}} = R_{t,i}^{\text{req}} \tag{4.5}$$

Case 3: Reservoir storage between the upper rule curve and the maximum storage

$$R_t^{\text{i}} = R_{t,i}^{\text{req}} + \left(S_t^{\text{i}} - S_{t,i}^{\text{upper}} \right) \leq R_i^{\max} \tag{4.6}$$

Case 4: Reservoir storage above the maximum storage

$$R_t^{\text{i}} = R_{t,i}^{\text{req}} + \left(S_t^{\text{i}} - S_i^{\max} \right) \tag{4.7}$$

Table 4.2 Physical reservoir constraints

Contents		Fanshawe	Wildwood	Pittock
Maximum Storage	Volume (10^3 m^3)	22,503	18,470	7,020
	Elevation (EL. M)	3.0	6.7	4.25
Minimum Storage	Volume (10^3 m^3)	5,500	2,430	0.0
	Elevation (EL. M)	-3.0	0.0	0.0

Table 4.3 Operational constraints of Wildwood and Pittock reservoirs (UTRCA, 1993)

Categories	Wildwood	Pittock
Flood control	- Not exceeding 10.0 m^3/s in most cases - Below a limit of 3.0 m^3/s to avoid nuisance flooding at the St. Mary's golf course	- No specific flood control flow target in the original operating rule - Potential backyard flooding of a property near Road 48 at flow of 40 m^3/s - Authority staff tend to moderate outflows to about 35 m^3/s
Low flow augmentation	- Target is 1.13 m^3/s - No reduction be acceptable	- Target is 0.42 m^3/s - No reduction be acceptable - The potential benefit from increased flows
Recreation	- Not fall below 1058 ft before Labour Day - Wide fluctuation over a short period should be avoided	- Minimizing over the summer
Fisheries	- Reach peak water levels by the end of the first week of April - Reduce peak water level during the spring period - Hold level stable at the summer level until late fall - Increase the minimum winter holding level	- Reach peak water levels by the end of the first week of April and should be held constant until mid-May - Water level should be lowered by about 1 m over a week period - Level should be held at the summer level with little fluctuation - Increase the minimum winter holding level up to 1.3 m (EL. 284.0)
Hydro power	- Reach peak water levels by the end of the first week of April	- No significant implications

where S_t^i represents the storage of reservoir i at the end of time t, $R_{t,i}^{req}$ is the required release from reservoir i during time t, the firm water supply from each reservoir, I_t^i is the inflow into reservoir i during time t, R_t^i is the release from reservoir i during time t, S_i^{min} is the minimum storage of reservoir i, S_i^{max} is the maximum storage of reservoir i, $S_{t,i}^{lower}$ is the lower rule curve of reservoir i at the time t, $S_{t,i}^{upper}$ is the upper rule curve of reservoir i at the time t, and R_i^{max} is the maximum release from reservoir i for reduction of flood damage.

Among three reservoirs in the Upper Thames River basin, the Fanshawe dam has the unique operational role - to keep the water elevation near the sill of dam (=EL. 0.0 m, storage volume = 12,350 × 10^3 m^3) most of the time. The reservoir gets filled only temporarily to manage floods. In this regard the Fanshawe reservoir is very different from the other two reservoirs, Wildwood and Pittock. It can release exactly what comes in (less the evaporation and other losses) maintaining the elevation of the sill of the dam and performing as a run-of-river dam unless there is a flood. In the case of flooding, the reservoir can store the inflows using the storage between the sill of dam and the maximum storage. Therefore, the lower and the upper rule curve are developed in this study to guide the optimal reservoir flood control operations. Equation (4.8) is used to distinguish between the release under normal and flooding conditions and determine the release ranges based on the flood damage as shown in Table 4.4:

$$R_t^i = S_{t-1}^i + I_t^i \; R_t^i - \text{sill of dam} \tag{4.8}$$

If R_t^i is less or equal to the maximum release 370 m^3/sec - non flooding conditions - the reservoir is operated as a run-of-river dam to maintain the sill of dam elevation all the time. However, if R_t^i is greater than 370 m^3/sec, the $R_{t,i}^{req}$ is set to the maximum release of 370 m^3/sec and reservoir storage S_t^i is

calculated using Eq. (4.3). The release calculation is performed using Eq. (4.9) to Eq. (4.12) according to the four possible situations as in the case of other two reservoirs.

Case 1**:** Reservoir storage below the lower rule curve (storing all surplus inflows in the reservoir)

$$R_t^{\mathrm{i}} = R_{t,i}^{\mathrm{req}} (= 370 \text{ m}^3/\text{sec}) \tag{4.9}$$

Case 2: Reservoir storage between the lower and the upper rule curve

$$R_t^{\mathrm{i}} = \{ R_t^{\mathrm{i}} (S_{t,i}^{\mathrm{upper}}) - R_t^{\mathrm{i}} (S_{t,i}^{\mathrm{lower}}) \} / (S_{t,i}^{\mathrm{upper}} - S_{t,i}^{\mathrm{lower}}) \times (S_t^{\mathrm{i}} - S_{t,i}^{\mathrm{lower}}) + R_t^{\mathrm{i}} (S_{t,i}^{\mathrm{upper}}) \tag{4.10}$$

Case 3: Reservoir storage between the upper rule curve and maximum storage

$$R_t^{\mathrm{i}} = R_{\mathrm{fld}}^{\max} (= 500 \text{ m}^3/\text{sec}) \tag{4.11}$$

Case 4: Reservoir storage above the maximum storage

$$R_i = R_{\mathrm{fld}}^{\max} + (S_t^{\mathrm{i}} - S_i^{\max}) \tag{4.12}$$

where $R_t^{\mathrm{i}} (S_{t,i}^{\mathrm{upper}})$ and $R_t^{\mathrm{i}} (S_{t,i}^{\mathrm{lower}})$ represent the release assigned to lower and upper rule curves, 400 m^3/sec and 500 m^3/sec, respectively. $R_{\mathrm{fld}}^{\max}$ represents the maximum release of 500 m^3/sec for flooding situation.

Note that the operation of Fanshawe reservoir according to the ending storage can be in: (1) the run-of-river mode, or (2) the flood control mode. The other two reservoirs are operated only in the flood control mode. The estimation of flood damage in this study is performed using Eq.(4.4) to Eq.(4.7) for the Wildwood and the Pittock reservoirs and Eq.(4.8) to Eq.(4.12) for the Fanshawe reservoir.

Table 4.4 The Fanshawe reservoir release ranges categorized by the flood damage

Releases (m^3/sec)		Action and impacts
0	370	No major flood effects
370	400	Commence monitoring
400	500	No further action
500	550	Areas around Adelaide and Kipps lane and Windermare and Adelaide overtopped
550	750	Adelaide street overtopping, possible evacuations
750	935	Serious flood damages
935		Broughdale dye breached

4.5 Results

In this chapter, a case study of the integrated reservoir management system is presented with three sets of scenarios as shown in Table 4.5. Case 1 provides application of scenario set Ⅰ generated with the original WG model with one variable (precipitation) and Case 2 presents two scenarios: 1) scenario set Ⅱ generated with original WG model with three variables named WG3 and 2) scenario set Ⅲ: generated with the modified WG that includes Principal Component Analysis and three variables WG-PCA3.

Table 4.5 Scenarios sets employed in the case study

Cases	Scenario set	WG model	Future scenarios generated
Case 1	Scenario set Ⅰ	WG model with one variable	Historic B21 B11
Case 2	Scenario set Ⅱ	WG3	
	Scenario set Ⅲ	WG-PCA3	

4.5.1 Case 1: WG weather scenarios (scenario set Ⅰ)

Sharif and Burn (2006) has developed the improved K-NN WG model with a perturbation process and applied it to the Upper Thames River basin to assess the impacts of climate change. Prodanovic and Simonovic (2006a, 2006b) have selected two GCMs that define the possible range of climate change impacts and employed them within the weather generator model as a dry scenario (called B11) and a wet scenario (called B21) to generate weather conditions (called scenario set Ⅰ) for 100 years in addition to the

third scenario that is based on the historic record. With generated weather scenarios, they have conducted the frequency analysis and concluded that more significant and frequent floods will occur in the basin.

The scenario set I is employed in this study with the proposed integrated reservoir management system to develop the optimal reservoir rule curves for each scenario. Each 100 years period is divided evenly into two parts: (a) development of the optimal operating rule curves (50 years); and (b) verification of the optimal operating rules by simulation (50 years). Fig. 4.7 to Fig. 4.9 show the optimal rule curves for B11(dry), B21(wet), and historic scenarios, respectively for all three reservoirs in the basin. Lower - DE and Upper - DE in these figures are denoting the lower and the upper optimal rule curves respectively, obtained using the differential evolution optimization algorithm imbedded in the integrated reservoir management system.

Compared with the current rule curves first, the optimal rule curves for Wildwood and Pittock have different tendency that maintain high storage during the wet period from November to February although the current rule curve maintains low storage to prepare flood events during that period. The objective function in this study includes only flood damage estimated by the amount of streamflow at the control points, however the current rule curves have developed with multi-objective function including required instream flows at the downstream, flood damage, and recreation. To decrease the flood damage at the downstream, therefore, the release should be decreased by storing the inflow in the reservoir. If there is no severe flood event during a specific period a rule curve would maintain high reservoir storage to decrease the flood damage. Based on the optimal rule curves for Wildwood and Pittock that show high storage during the wet period, therefore, it can be concluded that scenario set Ihas no severe flood event during the generated period. In addition, the optimal rule curve is developed on the basis of a scenario in DE algorithm. It makes the optimal solution sensitive to how deep and how often the flood events occur. If severe flood events occur in a specific month and no flood event in following month, therefore, the optimal rule curve may be presented with steep difference between two months, not smoothing the rule

curve. Therefore, the optimal rule curves show very higher storages and steep difference between months than the current rule curve.

The rule curves for three reservoirs under B11 (dry) climate change scenario show a tendency to store the inflow in reservoirs in order to decrease the downstream flood damage by maintaining the high reservoir levels over all periods. The optimal rule curve for B11 (dry) climate scenario for Wildwood reservoir is much higher than other rule curves and allows for storing more inflows during the period from August to December. Under the B11 (dry) climate scenario significant flooding will not occur during the period from August to December. On the other side, Pittock reservoir is showing a notable change in operation during the wet season, from January to March. According to the historic record, the floods often occur in February, so the rule curves for B11 (dry) climate scenario show a tendency in February to lower the reservoir storage and prepare for incoming significant flood flows. Since the maximum release flow for Pittock is 40.0 m^3/sec, during the simulation, the inflow surplus is stored in the reservoir if sufficient storage is available. If a reservoir does not have an enough space to store the flood waters, the surplus inflow must be released in the form of spill. The rule curves under B11 (dry) climate scenario still maintain the higher storage levels than the rule curves obtained under other scenarios. This is expected result, since the B11 as dry climate change scenario projects the decrease of inflow. On the other hand, the rule curves under B21 (wet) climate change scenario show the lowest storage levels in March, which demonstrates that the flood season under the wet climate change scenario is extended to start in March and the reservoir managers have to prepare the reservoirs for the flood control before March.

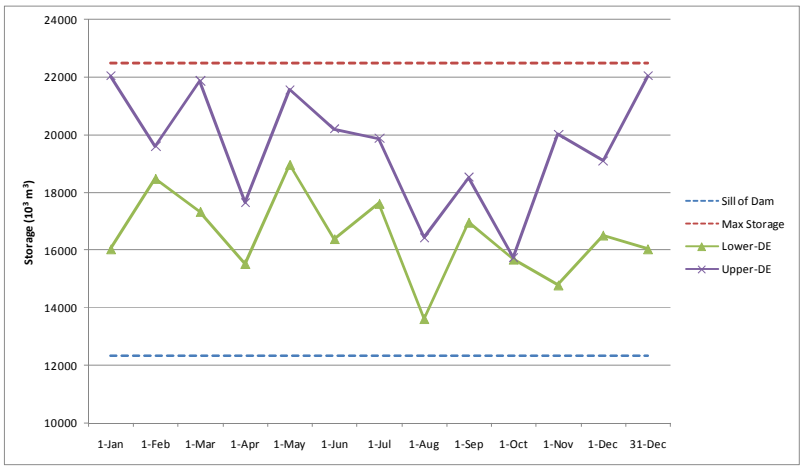

(a) B11 scenario

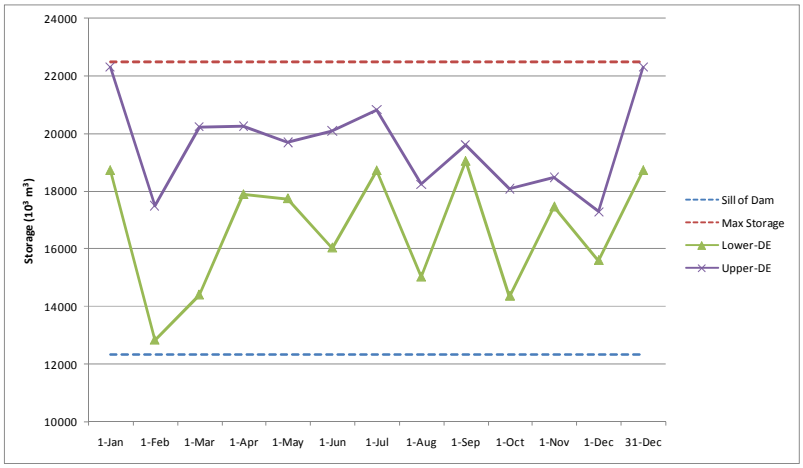

(b) B21 scenario

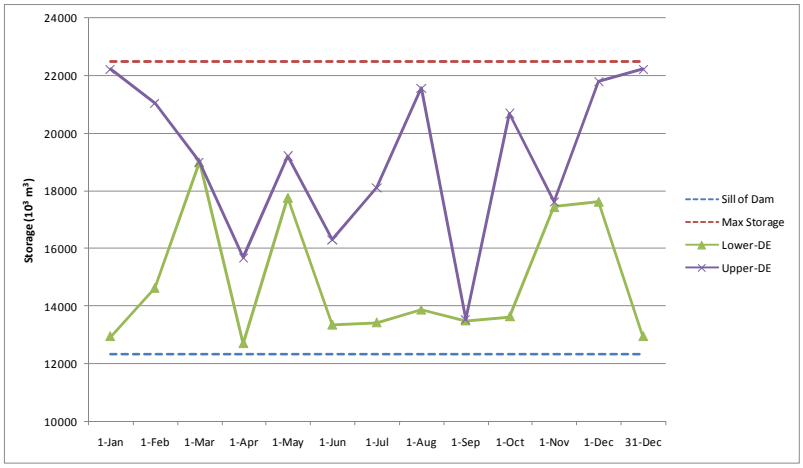

(c) Historic scenario

Figure 4.7 Optimal Fanshawe reservoir operating rule curves

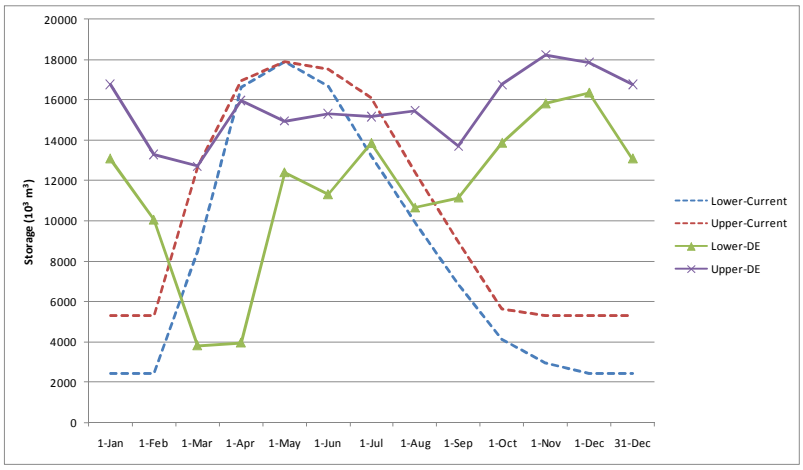

(a) B11 scenario

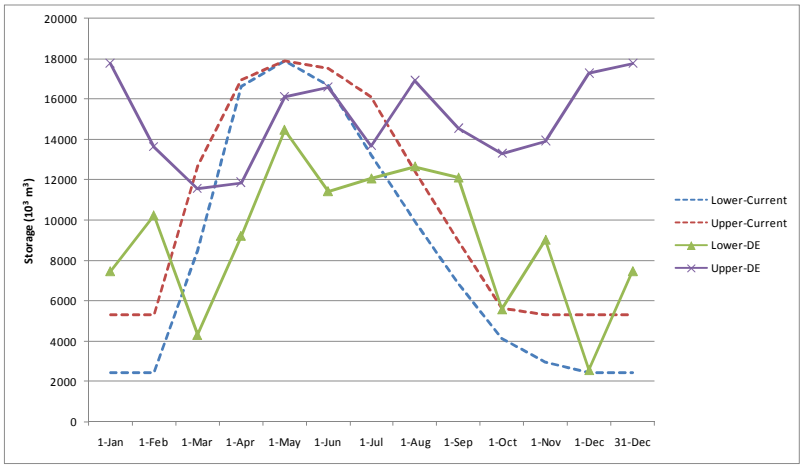

(a) B21 scenario

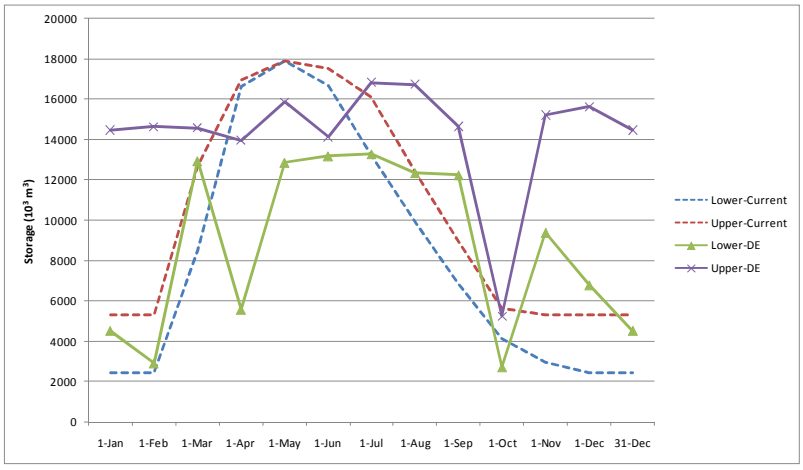

(c) Historic scenario

Figure 4.8 Optimal Wildwood reservoir operating rule curves

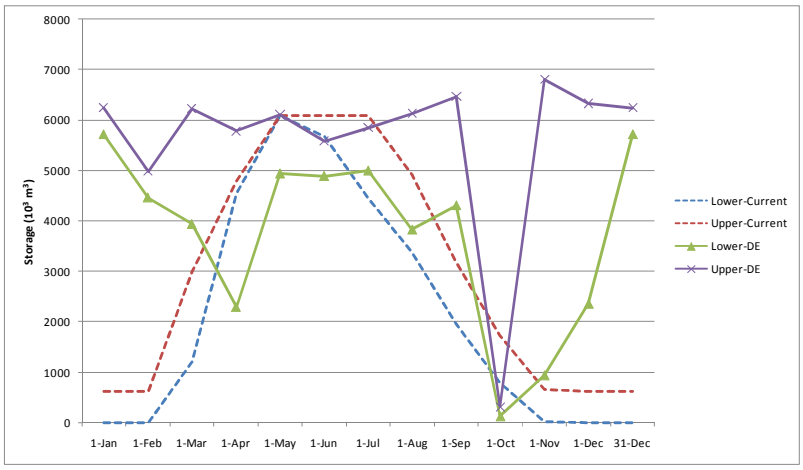

(a) B11 scenario

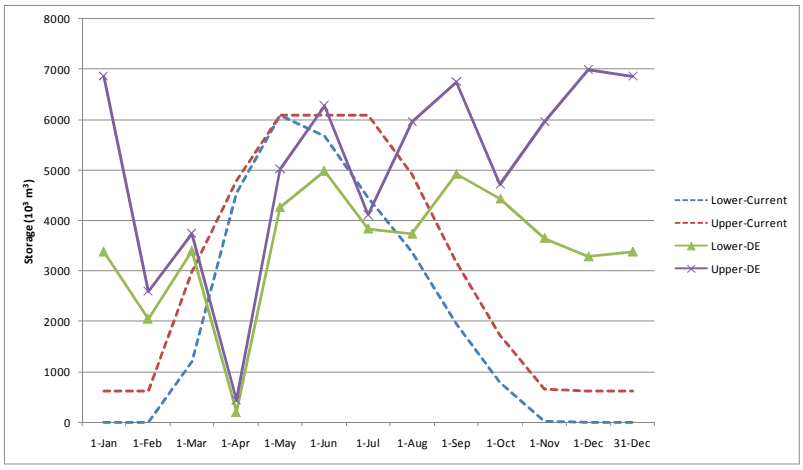

(b) B21 scenario

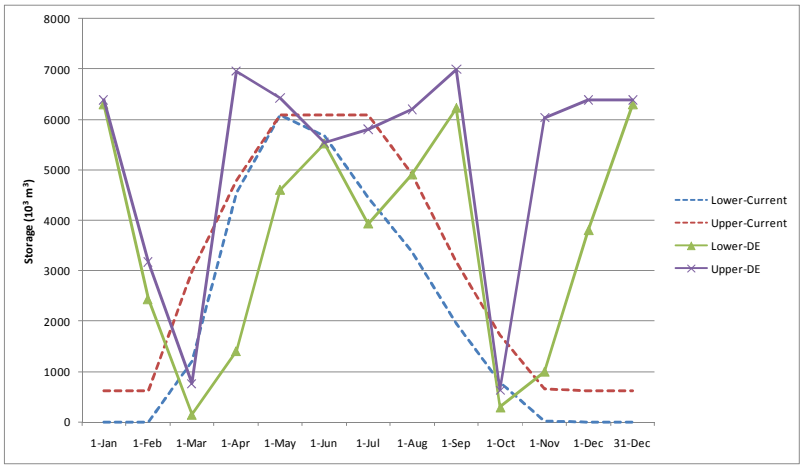

(c) Historic scenario

Figure 4.9 Optimal Pittock reservoir operating rule curves

The simulation of reservoir operations and corresponding flood damage calculations with three sets of rule curves developed for three different climate scenarios is performed in this study to verify the effects of the proposed optimal rule curves. Table 4.6 represents the yearly average flood damage calculated using the objective function as shown in Eq. (4.1). The each value of flood damage in the table represents the simulation result for a combination of climate scenario occurring in the future and one of the optimal rule curves developed in this study. For example, the value in the first cell, represents the total annual flood damage obtained with the rule curve developed assuming B11 scenario will occur and actually B11 scenario occurring in the future. Therefore, the values on the diagonal should show the best result in each column – the minimum flood damage. However, for B21 (wet) scenario, the rule curve developed with B11 (dry) scenario shows the minimum flood damage. Fig. 4.10 provides the daily reservoir storage for each climate scenario for 50 years of simulation. As pointed out earlier (Section 4.4.2), the Fanshawe reservoir is operated like run-of-river facility to maintain the sill of dam level ($12{,}349 \times 10^3$ m^3) if there are no significant floods. It is obvious, from the simulation results for scenario set I, that during the 50 years period no significant flood occurred. Therefore we conclude that the simulation period employed in this study is not sufficient to properly assess the effects of optimal reservoir operation on the flood damages in the basin. This explains the insignificant difference in level of flood damage as shown in Table 4.6. Due to lack of significant flood events in scenario set Iduring the simulation period, the optimal rule curve B11-DE obtained under B11 (dry) climates scenario, which stores more inflow in the reservoir, could be the best optimal operating policy even for B21 wet scenario - lower release from the reservoir decreases the total flood damage. Fig. 4.11 shows the streamflow at the Byron station where the two tributaries of the Thames River, the North Branch and the East Branch, join. The Byron station flows are affected by the operations of all three reservoirs in the basin. For the B21 (wet) scenario, the streamflow is highest in April. For the historic scenario the maximum streamflow occurs in February. This result demonstrates that obtaining the maximum space in all three reservoirs in March according to the optimal

B21-DE rule curve is appropriate in order to accommodate flood flows occurring in April.

Table 4.6 Yearly average flood damage (10^3 Canadian dollars/year)

Climate scenario / Rule curve	B11	B21	Historic
B11-DE	**6,382.0***	**7,390.9***	6,674.4
B21-DE	6,384.6	7,415.6	6,675.7
Historic-DE	6,384.8	7,419.0	**6,667.5***

* represents the best result among three rule curves for a scenario

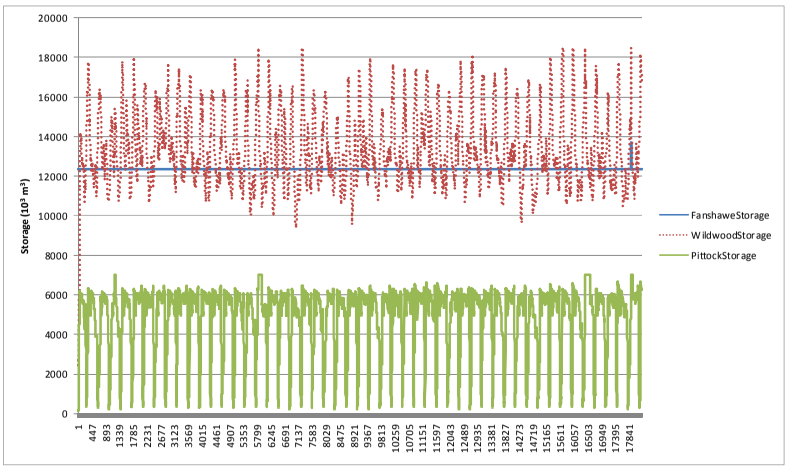

(a) B11 scenario

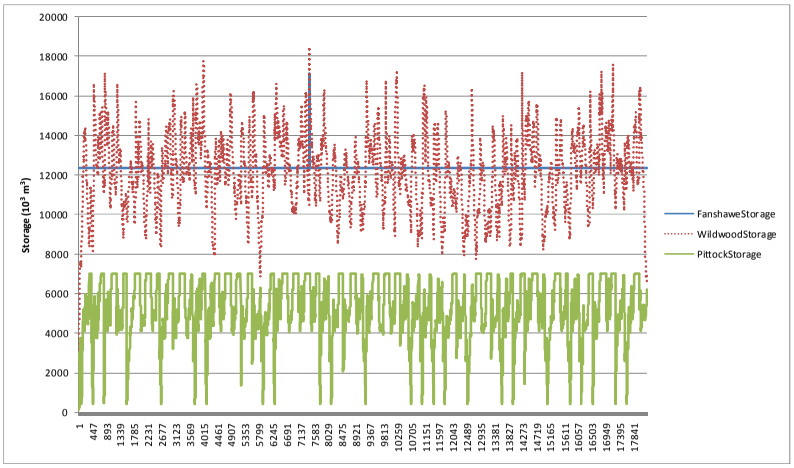

(b) B21 scenario

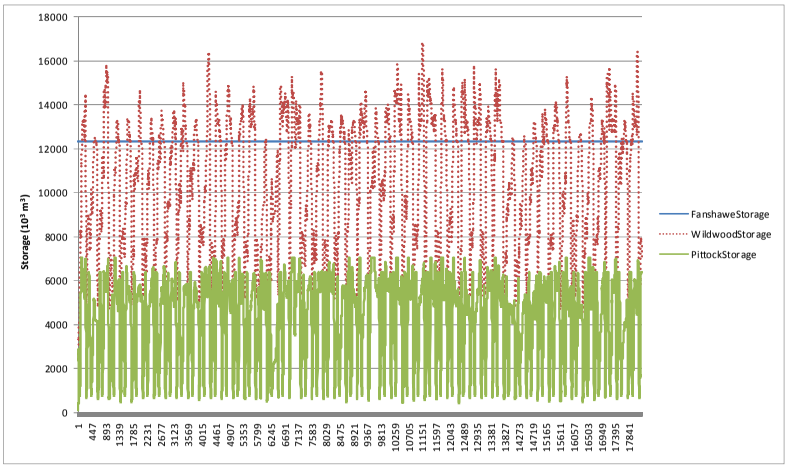

(c) Historic scenario

Figure 4.10 Daily reservoir storage for each climate scenario

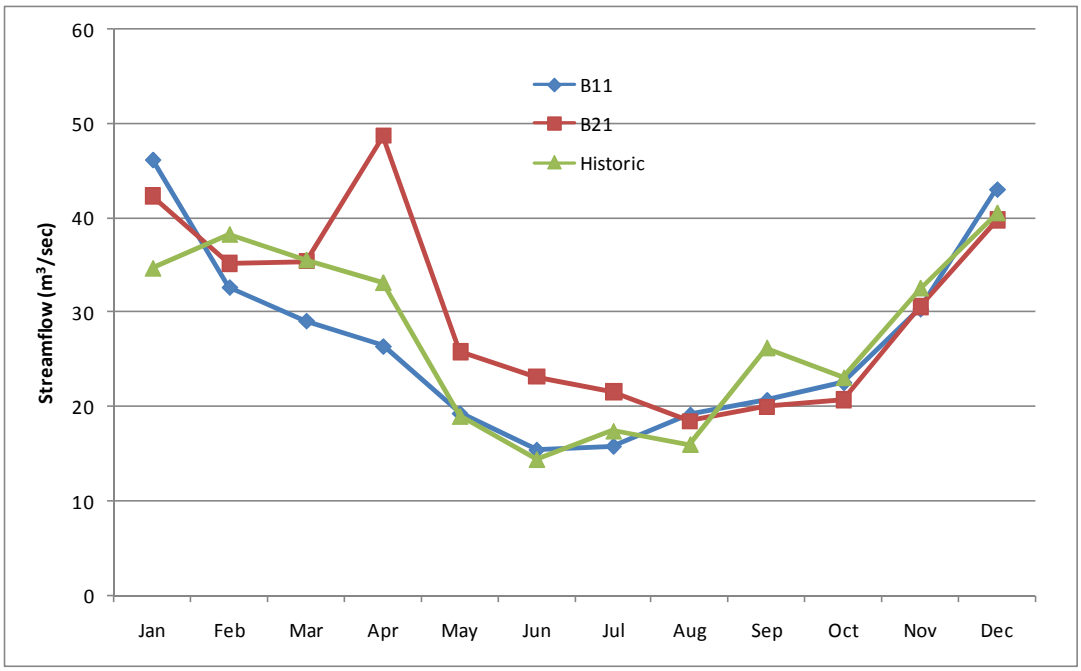

Figure 4.11 Streamflow at Byron station

4.5.2 Case 2: new weather scenarios generated by WG3 and WG-PCA3

The scenario set Ⅰdid not include enough significant flood events to assess the effects of the optimal reservoir operations on the flood damages under climatic change. Therefore, this study generates again the weather scenarios newly for 100 years to include more significant flood events using the original WG3 (scenario set Ⅱ)and WG-PCA3 (scenario set Ⅲ)described in Section 2.1 with three different weather scenario (B11, B21, and historic). In total, six future weather scenarios are generated and six sets of optimal reservoir operating rule curves are developed.

Fig. 4.12 to Fig. 4.14 show the rule curves for three climate scenarios (scenario set Ⅱ) obtained using the original WG3 model. Three rule curves for the Fanshawe reservoir provide for the conservative operating policies over the year (storing the inflows in the reservoir as much as possible). The B11-DE rule curve for the Wildwood reservoir is decreasing the storage in November in order to prepare for the upcoming wet season. The general tendency for B11 and historic scenarios is to keep the reservoir storage high. However, the B21-DE rule curves show low storage during the wet season - from December to March. Especially, the Wildwood reservoir rule curve is very low in March in order to prepare the reservoir for a significant incoming flood, while the Fanshawe reservoir (located below the Wildwood) rule curve is at the same time trying to store the inflows in the reservoir to decrease the downstream flood damages (e.g. Byron). This indicated that the Fanshawe reservoir still has capacity to control March flooding. For Pittock reservoir, located in upper region of the south branch, the B11-DE rule curves show are the lowest level for flood control in February. The other rule curves show the firm water supply release, or storing the inflows, during the summer season. In case of historic scenario, the reservoir operations for flood control are occurring from December to January in order to prepare sufficient storage in the reservoir for upcoming floods in February. Therefore, the rule curves in February show a wide range, between the lower and upper rule curves, of the firm water supply release during this period. The

B21-DE rule curves the show the low reservoir storage from February to April, which means the flood season is extended to April as in the first case, described in the previous section).

In addition, this study generated the weather scenarios (scenario set III)using the modified WG-PCA3 model and developed the rule curves shown in Fig. 4.15 to Fig. 4.17. First, the three optimal rule curves for the Fanshawe reservoir show the same tendency as the rule curves obtained using original WG3 model (storing the inflows in the reservoir as much as possible over a year). However, the Wildwood reservoir rule curves for B21 and historic climate scenarios show the reservoir operations expecting flooding from February to April. Similar to the original WG3 scenarios, the Wildwood reservoir rule curves show minimum storage in March – in the case of original WG3 scenarios the minimum was occurring from February to March, while Fanshawe reservoir is still storing the inflows in the reservoir to decrease the downstream flood damages. Therefore, these rule curves also demonstrate that the Fanshawe reservoir still has the capacity to control flooding during this period. The Pittock reservoir rule curves for B21 scenario prepare the reservoir for flood management in March, but that for historic scenario requires that the flood management is provided from February to April. These results are very interesting because the previous rule curves for the scenario set Iand the scenario set II show that the flood season would be extended up to April by B21 scenario as well as the scenario set III. However, historically the flood season is ended by February. Therefore, these results indicate that the flood operation should be extended to April if the B21 scenario occurs in the future.

With these six optimal reservoir rule curves for the scenario set IIand the scenario set III, this study simulates the reservoir performance and calculates the flood damage for 50 years using six future weather scenarios. Table 4.7 represents the yearly average flood damage calculated using the objective function and the bold results represent the best result among the six optimal rule curves for each weather scenario. Among the six optimal rule curves, the rule curve for B11(PCA) provides the best result for B11,

B11(PCA), and historic(PCA) scenarios and also the B21 rule curve represents the best results for B21 and B21(PCA). These results demonstrate that the DE optimization procedure performs very well and the optimal operating rule curves provide adequate adaptation of reservoir operations to changing climatic conditions.

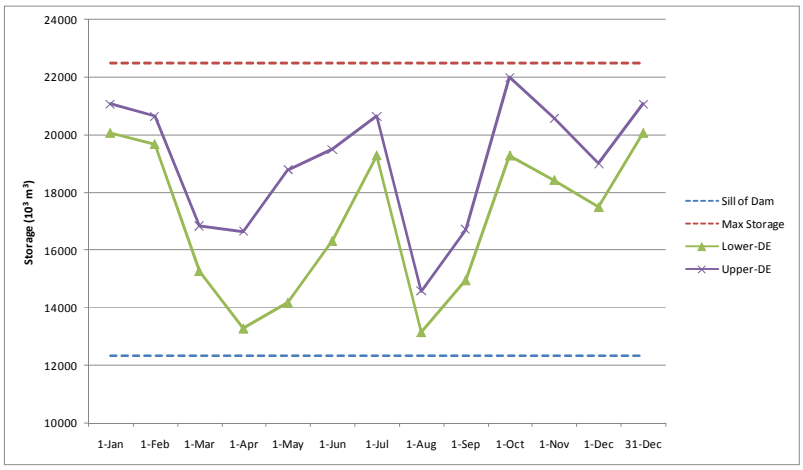

(a) B11 scenario

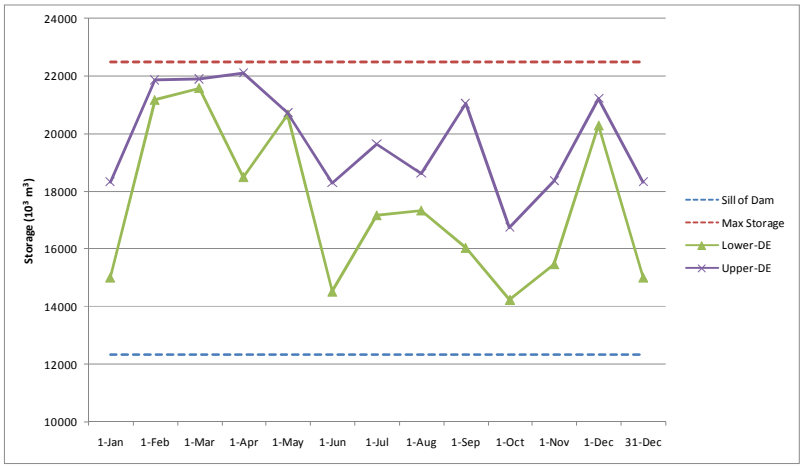

(b) B21 scenario

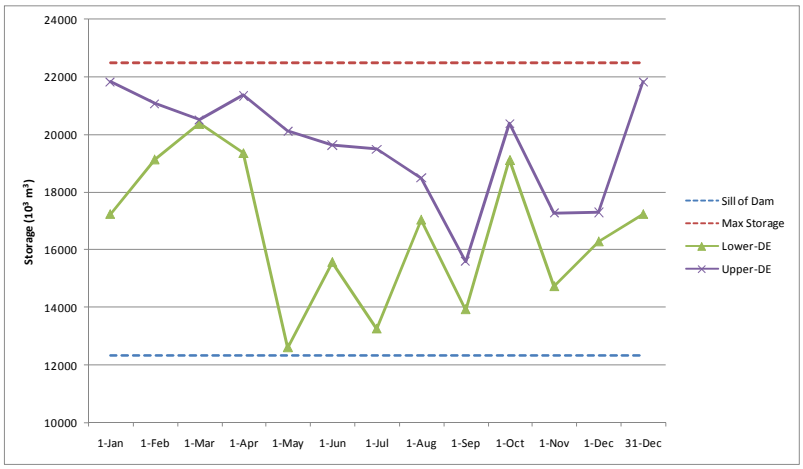

(c) Historic scenario

Figure 4.12 Optimal Fanshawe reservoir rule curves

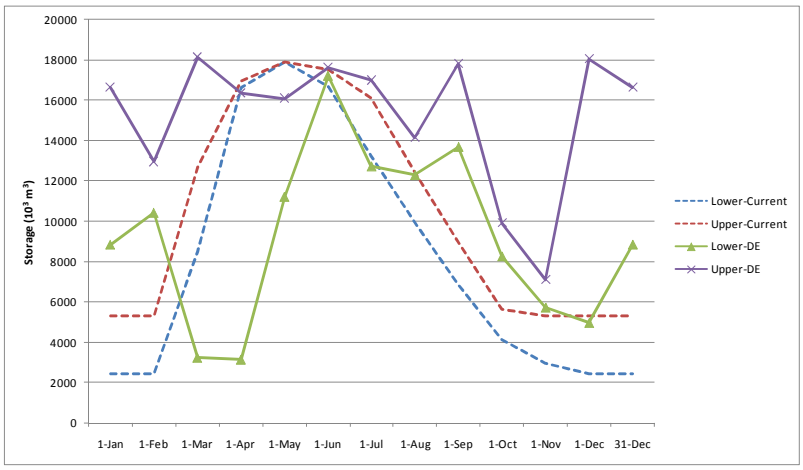

(a) B11 scenario

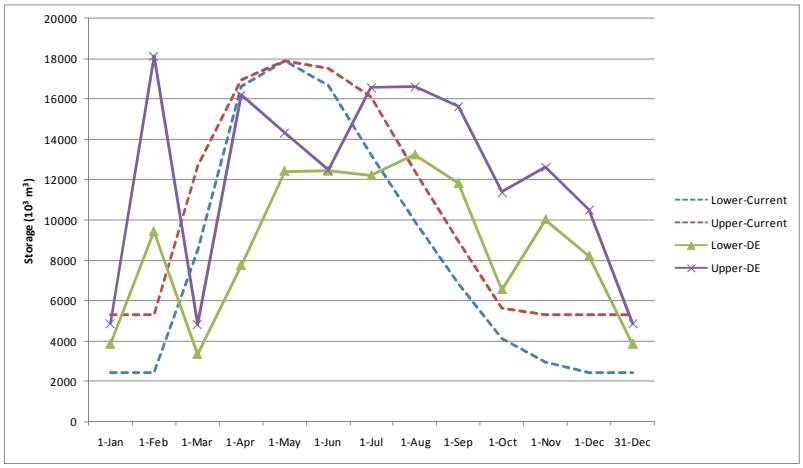

(a) B21 scenario

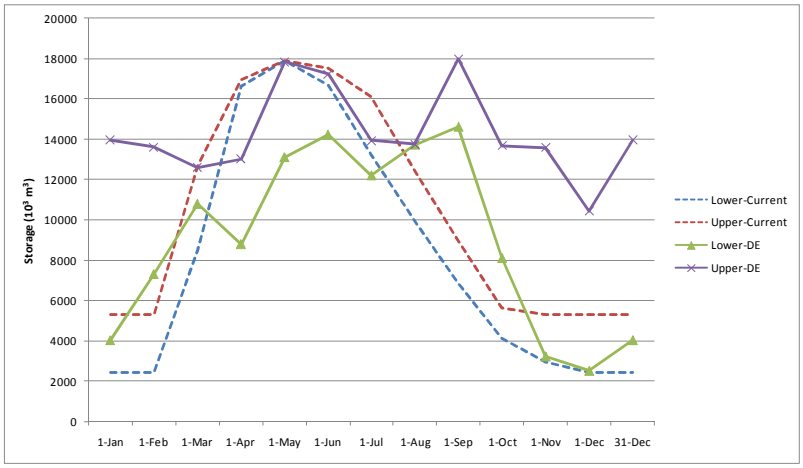

(c) Historic scenario

Figure 4.13 Optimal Wildwood reservoir rule curves

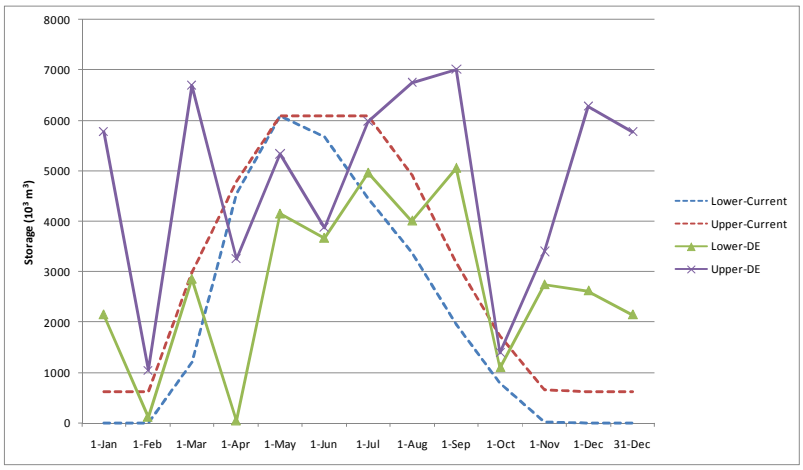

(a) B11 scenario

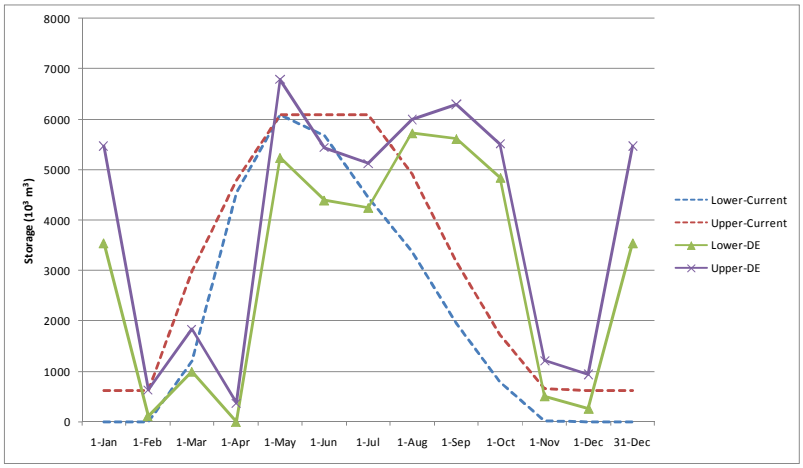

(b) B21 scenario

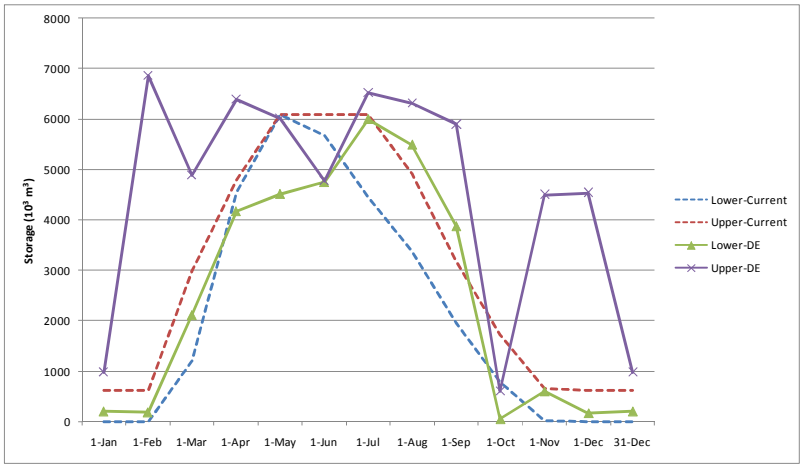

(c) Historic scenario

Figure 4.14 Optimal Pittock reservoir rule curves

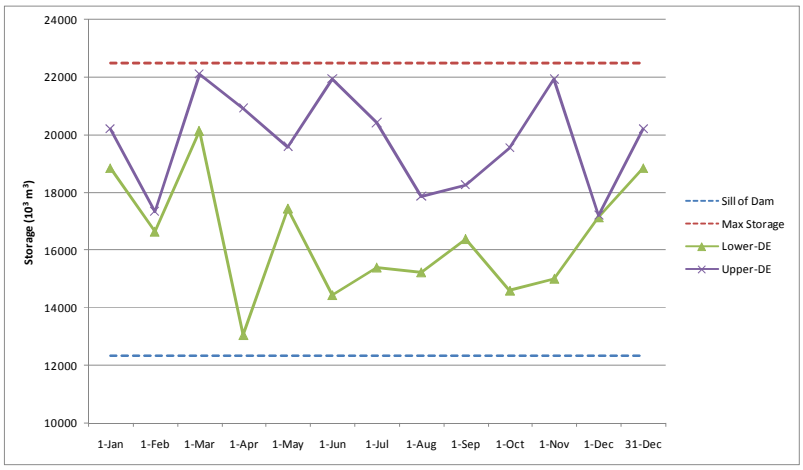

(a) B11-PCA scenario

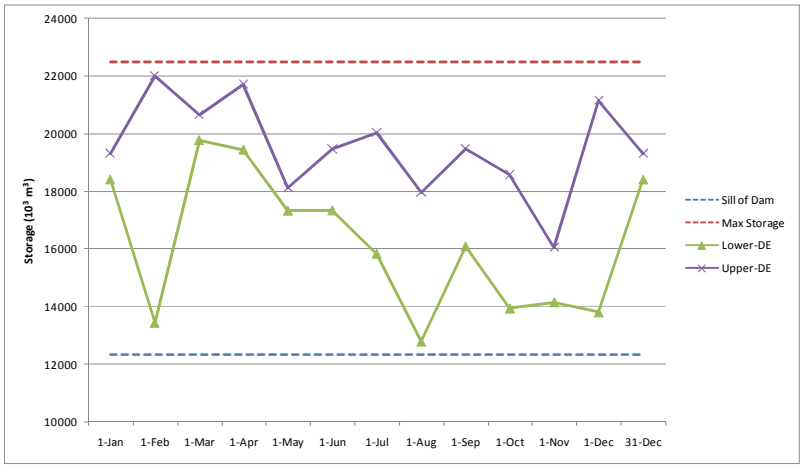

(b) B21-PCA scenario

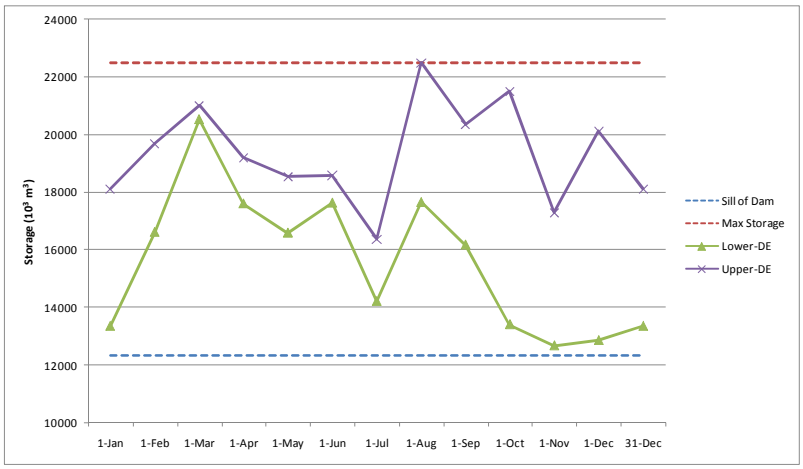

(c) Historic-PCA scenario

Figure 4.15 Optimal Fanshawe reservoir rule curves generated by WG-PCA3

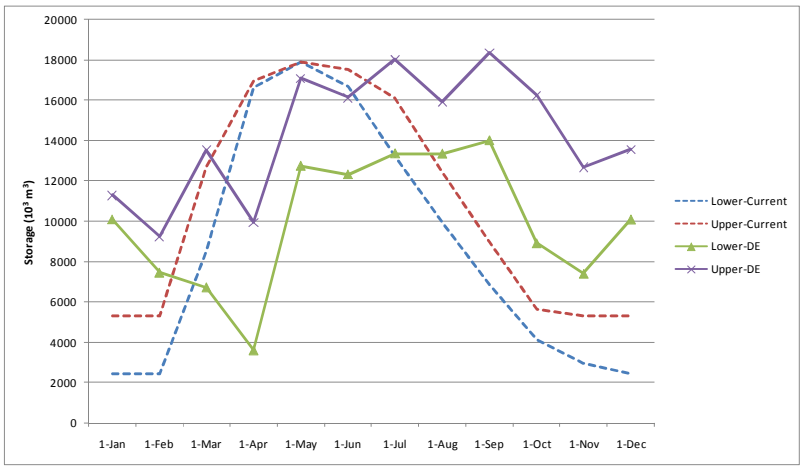

(a) B11-PCA scenario

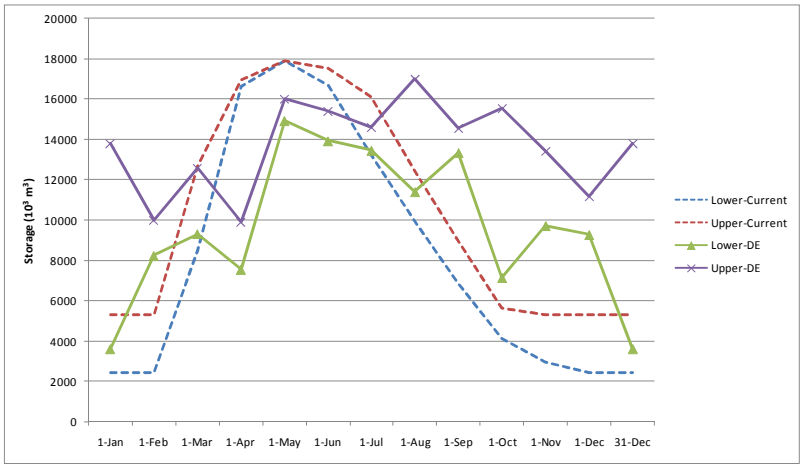

(a) B21-PCA scenario

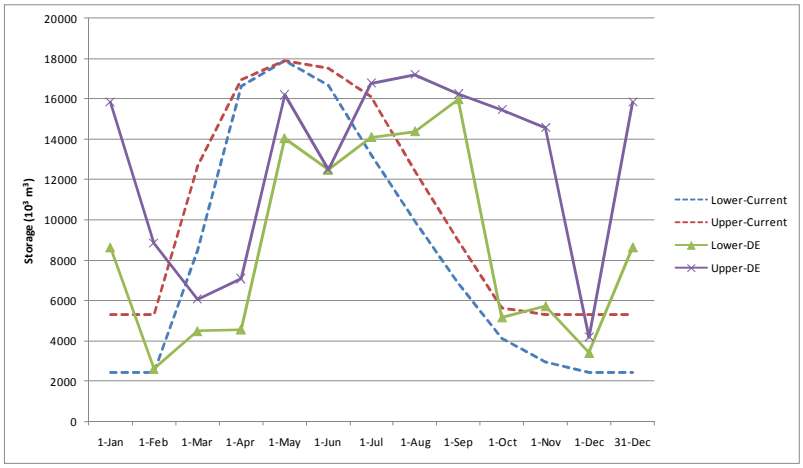

(c) Historic-PCA scenario

Figure 4.16 Optimal Wildwood reservoir rule curves generated by WG-PCA3

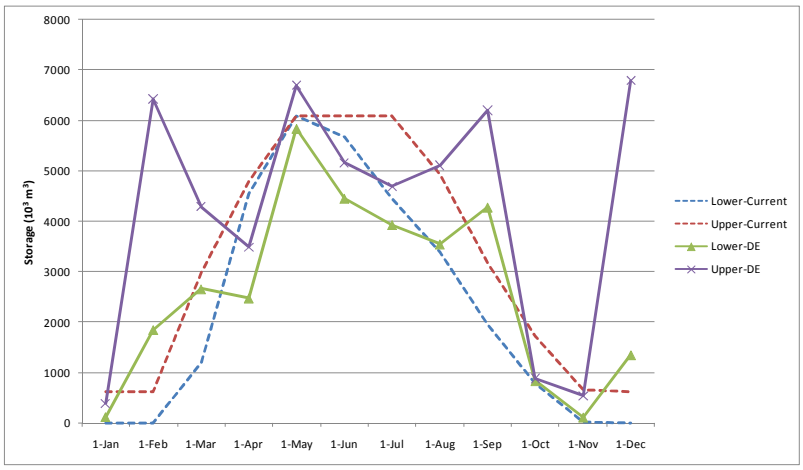

(a) B11 scenario

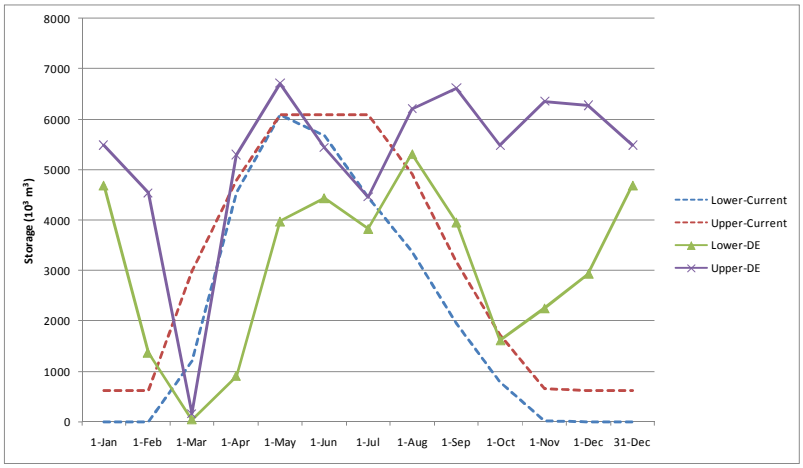

(b) B21 scenario

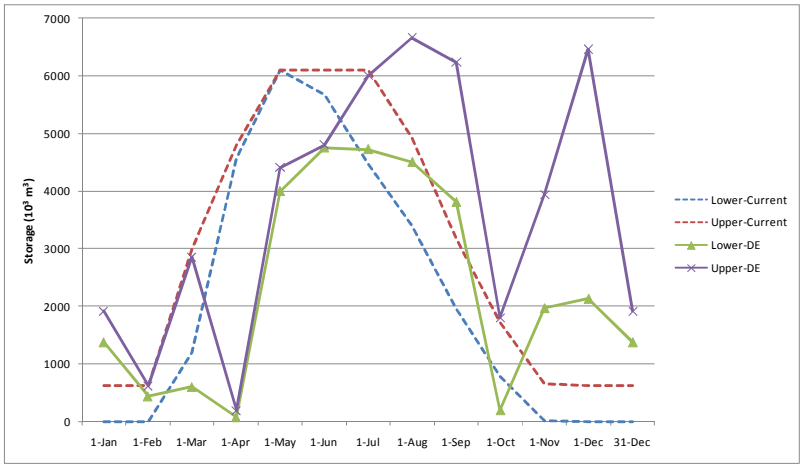

(c) Historic scenario

Figure 4.17 Optimal Pittock reservoir rule curves generated by WG-PCA 3

Table 4.7 Yearly average flood damage

Unit: 10^3 Canadian dollars/year

Rule curves	Climate scenario						Total flood damage
	B11	B11(PCA)	B21	B21(PCA)	Historic	Historic (PCA)	
B11	7,483.1	8,815.4	7,268.9	9,866.1	9,896.1	8,970.4	52,300.0
B11(PCA)	**7,451.3***	**8,799.8***	7,274.6	9,858.6	9,864.3	**8,935.8***	**52,184.4***
B21	7,480.7	8,849.2	**7,249.6***	**9,846.4***	9,909.8	8,958.1	52,293.8
B21(PCA)	7,517.5	8,893.4	7,253.1	9,910.4	9,965.2	8,999.4	52,539.0
Historic	7,471.9	8,818.8	7,278.6	9,984.9	**9,797.0***	9,090.9	52,442.1
Historic (PCA)	7,490.2	8,853.1	7,294.4	9,853.0	9,958.0	9,017.0	52,465.7

* represents the best result among three rule curves for a scenario

Fig. 4.18 shows the effect of B11 rule curves on flood damage in November at Byron. The reservoir storage is minimized by the end of October to make the space for upcoming flood during the wet season. By this rule curve, the reservoir storages at the beginning of November, especially the storage in the Wildwood reservoir, are lower than that for historic scenario as visible in Fig. 4.18. Therefore, when the flood occurs during the wet season, the flood damages are decreased for B11 scenario, compared to the damages for historic scenario. In Fig. 4.19 we see the reservoir storages and the flood damages for the B21 and historic rule curves at the Byron in April for B21 climate scenario. As mentioned before, the rule curves for B21 scenario tend to operate the reservoirs for flood control from December to April. Therefore, the storages of Wildwood and Pittock at the beginning of April for the B21 rule curves are lower than those for the historic scenario rule curves. As a result, the flood damage can be decreased by storing more inflows in the reservoirs during the period from December to April. In addition, Fig. 4.20 and Fig. 4.21 show the total flood damage during the period estimated in Fig. 4.18 and Fig. 4.19, respectively, at each control point considered in the objective function. As expected, the results with rule curves developed based on B11 and B21 scenarios show the decrease in flood damages at most control points for both B11 and B21 scenarios, compared to those obtained using the rule curves based on the historic climate scenario. Therefore, the total flood damage at each control point is decreased by the implementation of the optimal reservoir rule curve. In addition, this study found that the scenarios set III provide more wet weather conditions. Fig. 4.22 shows the monthly average streamflow at Byron station, for the scenario set II and III.

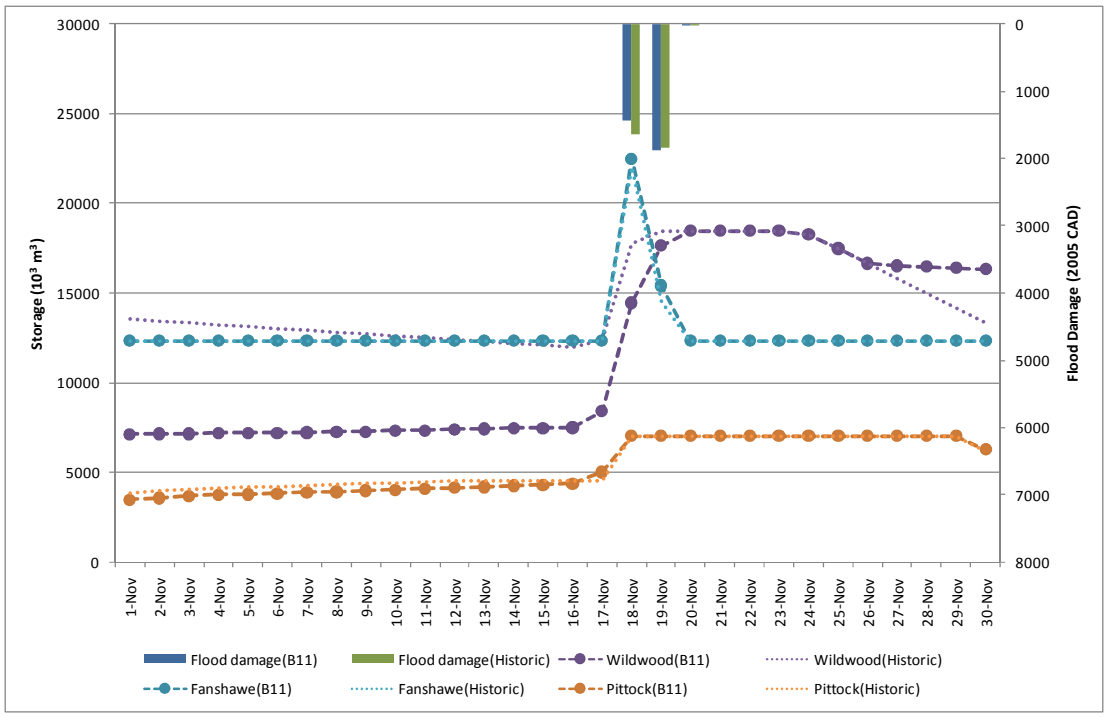

Figure 4.18 Reservoir storages and flood damages for the B11 and historic rule curves at the Byron in November for B11 scenario

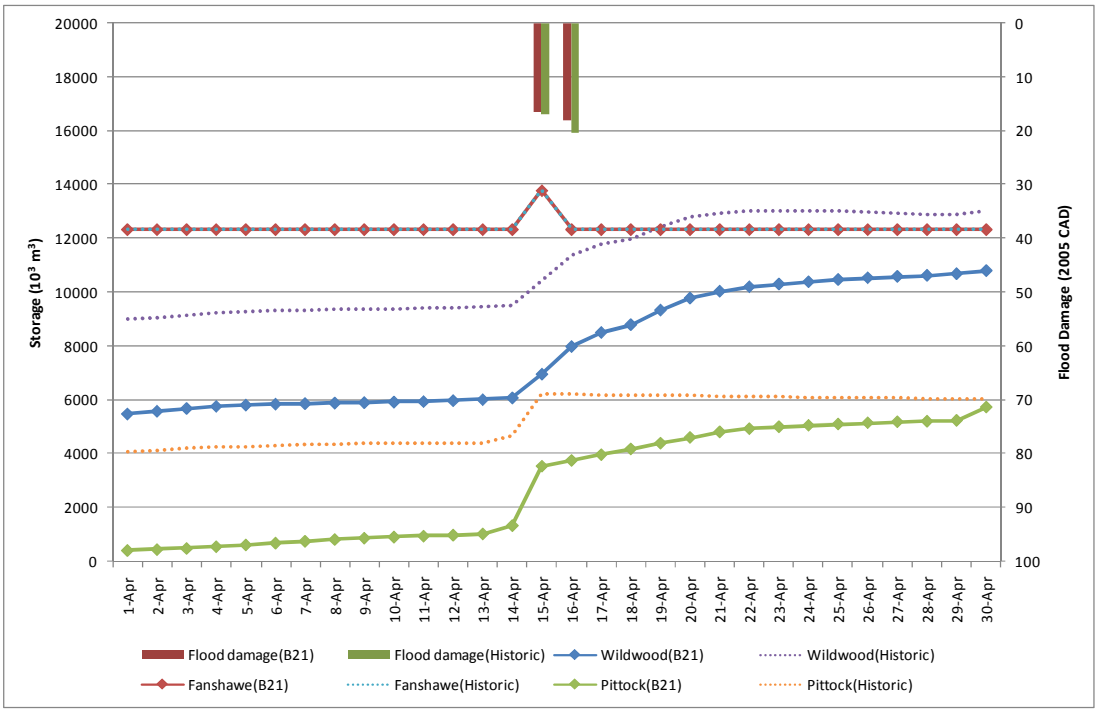

Figure 4.19 Reservoir storages and flood damages for the B21 and historic rule curves at the Byron in April for B21 scenario

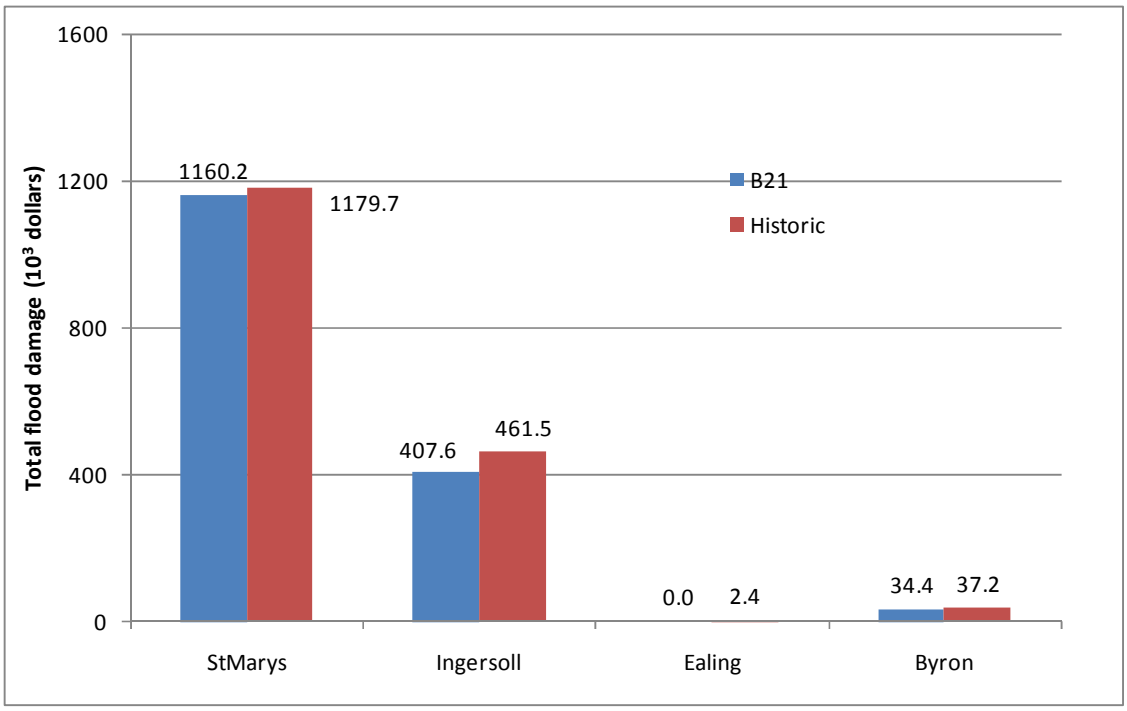

Figure 4.20 Total flood damages corresponding to the B21 rule curve and historic rule curve in April for B21 scenario

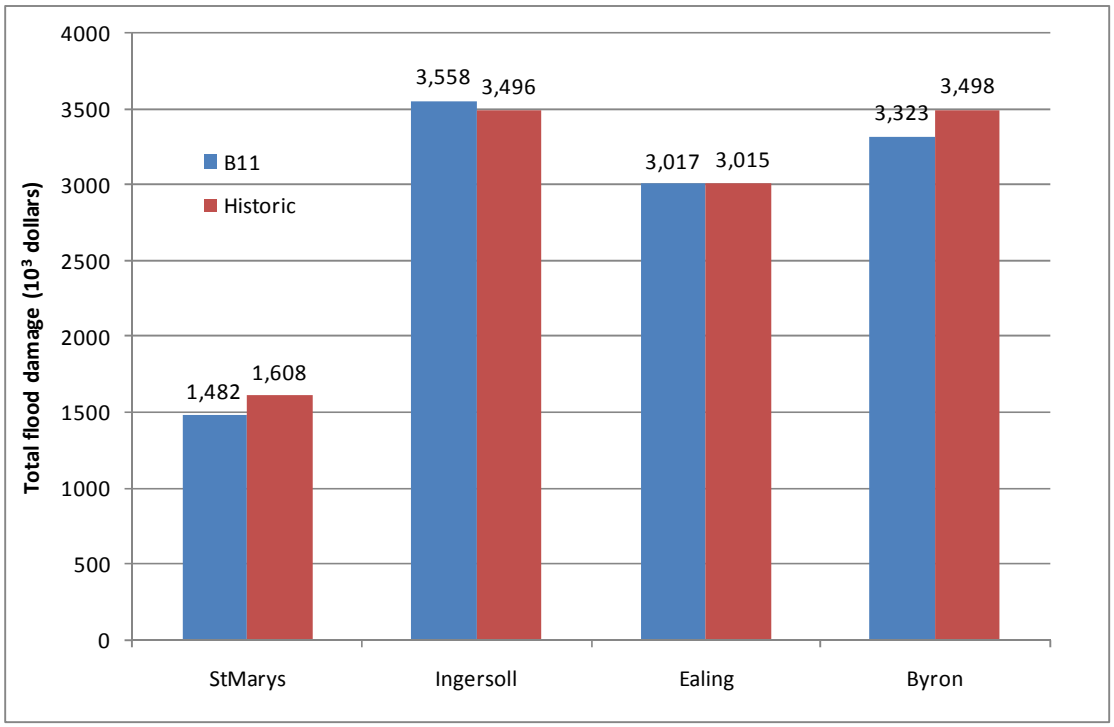

Figure 4.21 Total flood damages corresponding to the B11 rule curve and historic rule curve in November for B11 scenario

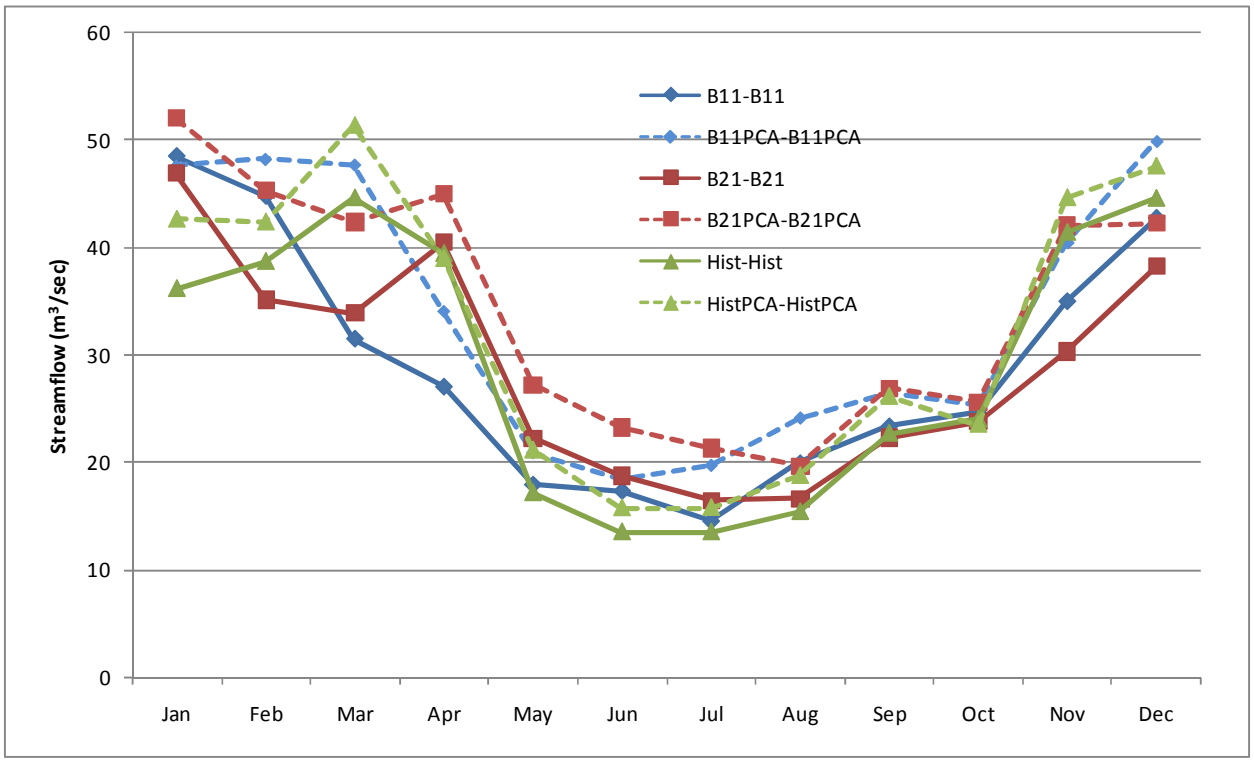

Figure 4.22 Streamflow at Byron corresponding to different rule curves and climate scenarios

5. Conclusion and future study outlook

This study presents an integrated reservoir management system for the Upper Thames River basin that includes: (1) a WG model; (2) a hydrological model; and (3) a differential evolutionary optimization model. The integrated reservoir management system is used to develop the optimal operating rule curves for three reservoirs in the basin that represent the best climate change adaptation strategy for existing storage in the basin. The original WG model is modified to add more variables available in the basin and generate the plausible weather conditions reflecting the available GCMs' outputs. The generated weather scenarios are used with the hydrological model to generate the streamflows according to the optimal reservoir operations provided by the optimization model. The optimization model generates randomly the alternatives based on the differential evolutionary algorithm and selects the optimal solution with the results calculated with the help of the hydrologic model.

Three different weather scenarios are employed to verify the integrated reservoir management system; (1) Case 1: scenarios set Ⅰ generated by the original WG model, and (2) Case 2: scenario set Ⅱand scenario set Ⅲ generated by WG3 and WG-PCA3, respectively. All weather scenarios and the developed rule curves (36 combinations - 6 rule curves × 6 scenarios = 36) are applied to each 50-year period to simulate basin response and calculate the total flood damages. The rule curves for B11 (dry) climate scenario provide a conservative reservoir operating policies, but show that earlier flood control operation is required, starting from October. For the B21 (wet) climate scenario, the flood management is required until April, which means that the flood season is extended to April. Historically the flood season ends in February. As expected, the rule curves for historic scenario require for flood management from December to February. In simulation results for the scenarios set Ⅰ , the B11 rule curves have a tendency of storing the inflows - the best result among three sets of the optimal rule curves because there is no significant

flood with three scenarios in this case. However, for the scenario set II and the scenario set III generated by WG3 and WG-PCA3, the B11 (PCA) rule curves provide the best result for B11, B11(PCA), and historic(PCA) scenarios and the B21 rule curves represent the best results for B21 and B21(PCA) scenarios. These results demonstrate that the DE optimization procedure performs very well to determine the best adaptation strategy to the climate change using existing storage in the basin. The total flood damages at each control point are decreased by the implementation of the optimal reservoir rule curves developed for various climate change scenarios. In addition, the WG-PCA3 provides more wet weather conditions than the original WG model.

The integrated reservoir management system proposed in this study provides the optimal reservoir operating rule curves that provide for adaptation to the climate change. The proposed system is flexible enough to accommodate more GCMs' results when available. The main advantage of the system is its flexible architecture that includes three different modules that can be easily revised when better tools become available.

Acknowledgments

This work was supported by the grant from the National Research Foundation of Korea (KRF-2007-357-D00258) and the grant from the Natural Sciences and Engineering Research Council of Canada.

References

Ahmad, S., and Simonovic, S. P. (2000). "System dynamics of reservoir operations for flood management." *Journal of Computational Civil Engineering*,4(3), 190–198.

Bardossy, A., Bogardi I., and Matyasovszky, I. (2005). "Fuzzy rule-based downscaling of precipitation." *Theoretical and Applied Climatology*, 82, 119–129.

Bennett, T. (1998). Development and application of a continuous soil moisture accounting algorithm for the Hydrologic Engineering Center Hydrologic Modeling System (HEC-HMS). Masters Thesis, Department of Civil and Environmental Engineering, University of California, Davis, California.

Buishand, T. A., and Brandsma, T. (2001). "Multisite simulation of daily precipitation and temperature in the Rhine Basin by nearest neighbor resampling." *Water Resources Research*, 37(11), 2761– 2776.

Burn, D. H. (1998). "Climatic change impacts on hydrological extremes and the implications for reservoirs." *Proc. Second Intl. Conf. on Climate and Water*, Espoo, Finland, 273–281.

Cannon, A. J., and Whitfield, P. H. (2002). "Downscaling recent stream flow conditions in British Columbia, Canada using ensemble neural network models." *Journal of Hydrology*, 259, 136–151.

Christensen, N. S., Wood, A. W., Voisin, N., Lettenmaier, D. P., and Palmer, R. N. (2004). "Effects of climate change on the hydrology and water resources of the Colorado River basin." *Climatic Change*, 62(1-3), 337-363.

Coulibaly, P., and Dibike, Y. B. (2004). *Downscaling of Global Climate Model Outputs for Flood Frequency Analysis in the Saguenay River System*. Final Project Report prepared for the Canadian Climate Change Action Fund, Environment Canada, Hamilton, Ontario, Canada.

Cunderlik, J. and Simonovic, S. P. (2004a). *Calibration, verification and sensitivity analysis of the HEC-HMS hydrologic model.* Water Resources Research Report no. 048, Facility for Intelligent Decision Support, Department of Civil and Environmental Engineering, London, Ontario, Canada.

Cunderlik, J. M., and Simonovic, S. P. (2004b). "Inverse modeling of water resources risk and vulnerability to changing climatic conditions." *Proceedings of the 57th Canadian Water Resources Association Annual Congress*. Water and Climate Change: Knowledge for Better Adaptation, CWRA, Montreal.

Cunderlik, J. M., and Simonovic, S. P. (2005). "Hydrological extremes in a south-western Ontario river basin under future climate conditions." *IAHS Hydrological Sciences Journal*, 50(4), 631-654.

Dorigo, M. (1992). Optimization, Learning and Natural Algorithms, PhD thesis, Politecnico di Milano, Italy.

Eberhart, R. C., and Kennedy, J. (1995). "A new optimizer using particle swarm theory." *Proceedings of the sixth international symposium on micro machine and human science*, IEEE service center, Piscataway, NJ, Nagoya, Japan, 39-43.

Goldberg, D. E. (1989). *Genetic Algorithms in Search, Optimization and Machine Learning*. Addison-Weseley.

Halland, J. H. (1975). *Adaptation in Natural and Artificial Systems*. The University of Michigan Press.

Hamlet, A. F., and Lettenmaier, D. P. (1999). "Effects of climate change on hydrology and water resources in the Columbia River Basin." *Journal of American Water Research Association*, 35(6), 1597-1623.

Hanson, C. L., and Johnson, G. L. (1998). *GEM (Generation of Weather Elements for Multiple Applications): Its Application in Areas of Complex Terrain*. In: Kovar, K., Tappeiner, U., Peters, N.E., Craig, R.G. (Eds.), Hydrology Water Resources and Ecology in Headwaters. International Association of Hydrological Sciences Press, Wallingford, 27–32.

Haylock, M. R., Cawley, G. C., Harpham, C., Wilby, R. L., and Goodess, C. M. (2006). "Downscaling heavy precipitation over the UK: A comparison of dynamical and statistical methods and their future scenarios." *International Journal of Climatology*, 26, 1397–1415.

IPCC (2000). *Special Report on Emissions Scenarios*. Cambridge University Press, Cambridge.

IPCC (2007). *Summary for Policymakers. Climate Change 2007: The physical science basis. Contribution of the Working Group I to the Fourth Assessment Report of the Intergovernmental Panel on Climate Change*. Cambridge University Press, Cambridge, United Kingdom.

Jones, P. D., Murphy, J. M., and Noguer, M. (1995). "Simulation of climate change over Europe using a nested regional-climate model. 1: Assessment of control climate, including sensitivity to location of lateral boundaries." *The Quarterly Journal of the Royal Meteorological Society*, 121, 1413–1449.

Kirkpatrick, S., Gelatt, C. D., and Vecchi, M. P. (1983). "Optimization by Simulated Annealing." *Science*, 220(4598), 671-680.

Kidson, J. W., and Thompson, C. S. (1998). "A comparison of statistical and model-based downscaling techniques for estimating local climate variations." *Journal of Climate*, 11, 735–753.

Kirshen, P. H., and Fennessey, N.M. (1995). Possible climate-change impacts on water supply of metropolitan Boston." *Journal of Water Resources Planning and Management*, 121(1), 61-70.

Labadie, J. W. (2004). "Optimal operation of multireservoir systems: State-of-the-art review." *Journal of Water Resources Planning and Management*, 130(2), 93-111.

Lall, U., and Sharma, A. (1996). "A nearest neighbour bootstrap for time series resampling." *Water Resources Research*, 32 (3), 679–693.

Lall, U., Rajagopalan, B., and Torboton, D. G., (1996). "A nonparametric wet/dry spell model for resampling daily precipitation." *Water Resources Research*, 32 (9), 2803–2823.

Lettenmaier, D. P., and Gan, T. Y. (1990). "An exploratory analysis of the hydrologic effects of global warming on the Sacramento-San Joaquin River basin, California." *Water Resources Research*, 26(1), 69-86.

Lettenmaier, D. P., Wood, A. W., Palmer, R. N., Wood, E. F., and Stakiv, E. Z. (1999). "Water resources implications of global warming: A U.S. regional perspective." *Climatic Change*, 43, 537-579.

Mehrotra, R; and Sharma, A. (2007). “Preserving low-frequency variability in generated daily rainfall sequences.” *Journal of Hydrology*, 345, 102-120.

Moscato, P. (1989). "On Evolution, Search, Optimization, Genetic Algorithms and Martial Arts: Towards Memetic Algorithms". *Caltech Concurrent Computation Program* (report 826).Nicks, A. D., Richardson, C. W., and Williams, J. R., (1990). “Evaluation of EPIC model weather generator: erosion/productivity impact calculator, 1. Model documentation.” In: Sharpley, A.N., Williams, J.R., (Eds.), *USDA-ARS Tech. Bull.*, 1768, 235.

Onwubolu, G. C., and Babu, B. V. (2004). *New Optimization Techniques in Engineering, Springer-Verlag*, Germany.

Parlange, M. B., and Katz, R. W. (2000). “An extended version of the Richardson model for simulating daily weather variables.” *Journal of Applied Meteorology*, 39, 610–622.

Payne, J. T., Wood, A. W., Hamlet, A. F., Palmer, R. N., and Lettenmaier, D. P. (2004). “Mitigating the effects of climate change on the water resources of the Columbia River basin.” *Climatic Change*, 62(1-3), 233-256.

Price, V. K., and Storn, M. R. (1997). “Differential evolution-A simple evoulution strategy for fast optimization.” *Dr. Dobb’s Journal*, 22, 18-24.

Price, V. K., Storn, M. R., and Lampinen, A. J. (2005). *Differential Evolution: A practical approach to global optimization*, Springer-Verlag Berlin, Heidelberg.

Prodanovic, P., and Simonovic, S. P. (2006a). *Inverse Flood Risk Modelling of The Upper Thames River Basin*, Water Resources Research Report no. 052, Facility for Intelligent Decision Support, Department of Civil and Environmental Engineering, London, Ontario, Canada.

Prodanovic, P., and Simonovic, S. P. (2006b). *Inverse Drought Risk Modelling of The Upper Thames River Basin*, Water Resources Research Report no. 053, Facility for Intelligent Decision Support, Department of Civil and Environmental Engineering, London, Ontario, Canada.

Prodanovic, P. and Simonovic, S. P. (2007). "Impacts of changing climatic conditions in the Upper Thames River Basin." *Canadian Water Resources Journal*, 32(4), 1-19.

Prudhomme, C., Jakob, D., and Svensson, C. (2003). "Uncertainty and climate change impact on the flood regime of small UK catchments." *Journal of Hydrology*, 277, 1 –23.

Rajagopalan, B., and Lall, U. (1999). "A k-nearest neighbour simulator for daily precipitation and other variables." *Water Resources Research*, 35(10), 3089–3101.

Rao, S. S. (1996). *Engineering optimization*, John Wiley & Sons, NY.

Simonovic, S. P., and Li, L. (2003). "Methodology for assessment of climate change impacts on large-scale flood protection system." *Journal of Water Resources Planning Management*, 129(5), 361–371.

Salathé, E. P. (2004). "Methods for selecting and downscaling simulations of future global climate with application to hydrologic modeling." *International Journal of Climatology*, 25, 419-436.

Sharif, M., and Burn, D. H. (2006). "Simulating climate change scenarios using an improved K-nearest neighbor model." *Journal of Hydrology*, 325, 179-196.

Sharma, A., Tarboton, D. G., and Lall, U. (1997). "Streamflow simulation: A nonparametric approach." *Water Resources Research*, 33(2), 291-308.

Simonovic, S. P., and Li, L. (2004). "Sensitivity of the red river basin flood protection system to climate variability and change." *Water Resources Management*, 18, 89–110.

Smith J. B., and Tirpak, D. A. (1989). *The Potential Effects of Global Climate Change on the United States*, Office of Policy, Planning, and Evaluation, USEPA, Washington D.C., USA.

Tripathi, S., and Srinivas, V. V. (2005). "Downscaling of general circulation models to assess the impact of climate change on rainfall of India." *Proceedings of International Conference on Hydrological Perspectives for Sustainable Development (HYPESD -2005)*, 23– 25 February, IIT Roorkee, India, 509–517.

Payne, J. T., Wood, A. W., Hamlet, A. F., Palmer, R. N., and Lettenmaier, D. P. (2004). "Mitigating the effects of climate change on the water resources of the Columbia River basin." *Climatic Change*, 62(1-3), 233-256.

UTRCA (1993). *Low Flow Hydrology and Operations Optimization Study. Wildwood and Pittock Reservoirs*. Final Report.

UTRCA (2005). *Flood Damage Estimation in the Upper Thames River Watershed: Assessment of Water Resources Risk and Vulnerability to Changing Climatic Conditions*, Project report VII.

VanRheenen, N. T., Wood, A. W., Palmer, R. N., and Lettenmaier, D.P. (2004). "Potential implications of PCM climate change scenarios for Sacramento-San Joaquin River basin hydrology and water resources." *Climatic Change*, 62(1-3), 257-281.

Westmacott, J. R., and Burn, D. H. (1997). "Climate change effects on the hydrological regime within the Churchill–Nelson river Basin." *Journal of Hydrology*, 202, 263–279.

Widmann, M., Bretherton, C. S., and Salathé, E. P. (2003). "Precipitation downscaling over the Northwestern United States using numerically simulated precipitation as a predictor." *Journal of Climate*, 16(5), 799-816.

Wilby, R. L., Hassan, H., and Hanaki, K. (1998). "Statistical downscaling of hydrometeorological variables using general circulation model output." *Journal of Hydrology*, 205, 1–19.

Wilby, R. L., Hay, L. E., Gutowski, W. J., Arritt, R. W., Takle, E. S., Pan, Z. T., Leavesley, G.H., and Clark, M.P. (2000). "Hydrological responses to dynamically and statistically downscaled climate model output." *Geophysical Research Letters*, 27(8), 1199–1202.

Wilcox, I., Quinlan, C., Rogers, C., Troughton, M., McCallum, I., Quenneville, A., Heagy, E., and Dool, D. (1998). *The Thames River Watershed: A Background Study for Nomination under the Canadian Heritage Rivers System*. Upper Thames River Conservation Authority, London, Ontario, Canada.

Wilks, D. S., and Wilby, R. L. (1999). "The weather generation game: a review of stochastic weather models." *Progress in Physical Geography*, 23(3), 329-357.

Wood, A. W., Maurer, E. P., Kumar, A., and Lettenmaier, D. P. (2002). "Long range experimental hydrologic forecasting for the eastern U.S." *Journal of Geophysical Research*, 107(D20), 4429.

Yates, D., Gangopadhyay, S., Rajagopalan, B., and Strzepek, K. (2003). "A technique for generating regional climate scenarios using a nearest-neighbor algorithm." *Water Resources Research*, 39(7), SWC 7-1–SWC 7-14.

Yeh, W. W-G. (1985). "Reservoir management and operations models: a state-of-the-art review." *Water Resources Research*, 21(12), 1797-1818.

Young, K.C. (1994). "A multivariate chain model for simulating climatic parameters with daily data." *Journal of Applied Meteorology*, 33, 661–671.

Appendix 1

Previous Reports in the Series

ISSN: (print) 1913-3200; (online) 1913-3219

1. Slobodan P. Simonovic (2001). Assessment of the Impact of Climate Variability and Change on the Reliability, Resiliency and Vulnerability of Complex Flood Protection Systems. Water Resources Research Report no. 038, Facility for Intelligent Decision Support, Department of Civil and Environmental Engineering, London, Ontario, Canada, 91 pages. ISBN: (print) 978-0-7714-2606-3; (online) 978-0-7714-2607-0.

2. Predrag Prodanovic (2001). Fuzzy Set Ranking Methods and Multiple Expert Decision Making. Water Resources Research Report no. 039, Facility for Intelligent Decision Support, Department of Civil and Environmental Engineering, London, Ontario, Canada, 68 pages. ISBN: (print) 978-0-7714-2608-7; (online) 978-0-7714-2609-4.

3. Nirupama and Slobodan P. Simonovic (2002). Role of Remote Sensing in Disaster Management. Water Resources Research Report no. 040, Facility for Intelligent Decision Support, Department of Civil and Environmental Engineering, London, Ontario, Canada, 107 pages. ISBN: (print) 978-0-7714-2610-0; (online) 978-0-7714- 2611-7.

4. Taslima Akter and Slobodan P. Simonovic (2002). A General Overview of Multiobjective Multiple-Participant Decision Making for Flood Management. Water Resources Research Report no. 041, Facility for Intelligent Decision Support, Department of Civil and Environmental Engineering, London, Ontario, Canada, 65 pages. ISBN: (print) 978-0-7714-2612-4; (online) 978-0-7714-2613-1.

5. Nirupama and Slobodan P. Simonovic (2002). A Spatial Fuzzy Compromise Approach for Flood Disaster Management. Water Resources Research Report no. 042, Facility for Intelligent Decision Support, Department of Civil and Environmental Engineering, London, Ontario, Canada, 138 pages. ISBN: (print) 978-0-7714-2614-8; (online) 978-0-7714-2615-5.

6. K. D. W. Nandalal and Slobodan P. Simonovic (2002). State-of-the-Art Report on Systems Analysis Methods for Resolution of Conflicts in Water Resources Management. Water Resources Research Report no. 043, Facility for Intelligent Decision Support, Department of Civil and Environmental Engineering, London, Ontario, Canada, 216 pages. ISBN: (print) 978-0-7714-2616-2; (online) 978-0-7714-2617-9.

7. K. D. W. Nandalal and Slobodan P. Simonovic (2003). Conflict Resolution Support System – A Software for the Resolution of Conflicts in Water Resource Management. Water Resources Research Report no. 044, Facility for Intelligent Decision Support, Department of Civil and Environmental Engineering, London, Ontario, Canada, 144 pages. ISBN: (print) 978-0-7714-2618-6; (online) 978-0-7714-2619-3.

8. Ibrahim El-Baroudy and Slobodan P. Simonovic (2003). New Fuzzy Performance Indices for Reliability Analysis of Water Supply Systems. Water Resources Research Report no. 045, Facility for Intelligent Decision Support, Department of Civil and Environmental Engineering, London, Ontario, Canada, 90 pages. ISBN: (print) 978- 0-7714-2620-9; (online) 978-0-7714-2621-6.

9. Juraj Cunderlik (2003). Hydrologic Model Selection for the CFCAS Project: Assessment of Water Resources Risk and Vulnerability to Changing Climatic Conditions. Water Resources Research Report no. 046, Facility for Intelligent Decision Support, Department of Civil and Environmental Engineering, London, Ontario, Canada, 40 pages. ISBN: (print) 978-0-7714-2622-3; (online) 978-0-7714- 2623-0.

10. Juraj Cunderlik and Slobodan P. Simonovic (2004). Selection of Calibration and Verification Data for the HEC-HMS Hydrologic Model. Water Resources Research Report no. 047, Facility for Intelligent Decision Support, Department of Civil and Environmental Engineering, London, Ontario, Canada, 29 pages. ISBN: (print) 978- 0-7714-2624-7; (online) 978-0-7714-2625-4.

11. Juraj Cunderlik and Slobodan P. Simonovic (2004). Calibration, Verification and Sensitivity Analysis of the HEC-HMS Hydrologic Model. Water Resources Research Report no. 048, Facility for Intelligent Decision Support, Department of Civil and Environmental Engineering, London, Ontario, Canada, 113 pages. ISBN: (print) 978- 0-7714-2626-1; (online) 978-0-7714-2627-8.

12. Predrag Prodanovic and Slobodan P. Simonovic (2004). Generation of Synthetic Design Storms for the Upper Thames River basin. Water Resources Research Report no. 049, Facility for Intelligent Decision Support, Department of Civil and Environmental Engineering, London, Ontario, Canada, 20 pages. ISBN: (print) 978- 0-7714-2628-5; (online) 978-0-7714-2629-2.

13. Ibrahim El-Baroudy and Slobodan P. Simonovic (2005). Application of the Fuzzy Performance Indices to the City of London Water Supply System. Water Resources Research Report no. 050, Facility for Intelligent Decision Support, Department of Civil and Environmental Engineering, London, Ontario, Canada, 137 pages. ISBN: (print) 978-0-7714-2630-8; (online) 978-0-7714-2631-5.

14. Ibrahim El-Baroudy and Slobodan P. Simonovic (2006). A Decision Support System for Integrated Risk Management. Water Resources Research Report no. 051, Facility for Intelligent Decision

Support, Department of Civil and Environmental Engineering, London, Ontario, Canada, 146 pages. ISBN: (print) 978-0-7714-2632-2; (online) 978-0-7714-2633-9.

15. Predrag Prodanovic and Slobodan P. Simonovic (2006). Inverse Flood Risk Modelling of The Upper Thames River Basin. Water Resources Research Report no. 052, Facility for Intelligent Decision Support, Department of Civil and Environmental Engineering, London, Ontario, Canada, 163 pages. ISBN: (print) 978-0-7714-2634-6; (online) 978-0-7714-2635-3.

16. Predrag Prodanovic and Slobodan P. Simonovic (2006). Inverse Drought Risk Modelling of The Upper Thames River Basin. Water Resources Research Report no. 053, Facility for Intelligent Decision Support, Department of Civil and Environmental Engineering, London, Ontario, Canada, 252 pages. ISBN: (print) 978-0-7714-2636-0; (online) 978-0-7714-2637-7.

17. Predrag Prodanovic and Slobodan P. Simonovic (2007). Dynamic Feedback Coupling of Continuous Hydrologic and Socio-Economic Model Components of the Upper Thames River Basin. Water Resources Research Report no. 054, Facility for Intelligent Decision Support, Department of Civil and Environmental Engineering, London, Ontario, Canada, 437 pages. ISBN: (print) 978-0-7714-2638-4; (online) 978- 0-7714-2639-1.

18. Subhankar Karmakar and Slobodan P. Simonovic (2007). Flood Frequency Analysis Using Copula with Mixed Marginal Distributions. Water Resources Research Report no. 055, Facility for Intelligent Decision Support, Department of Civil and Environmental Engineering, London, Ontario, Canada, 144 pages. ISBN: (print) 978- 0-7714-2658-2; (online) 978-0-7714-2659-9.

19. Jordan Black, Subhankar Karmakar and Slobodan P. Simonovic (2007). A Web- Based Flood Information System. Water Resources Research Report no. 056, Facility for Intelligent Decision Support, Department of Civil and Environmental Engineering, London, Ontario, Canada, 133 pages. ISBN: (print) 978-0-7714-2660-5; (online) 978-0-7714-2661-2.

20. Angela Peck, Subhankar Karmakar and Slobodan P. Simonovic (2007). Physical, Economical, Infrastructural and Social Flood Risk – Vulnerability Analyses in GIS. Water Resources Research Report no. 057, Facility for Intelligent Decision Support, Department of Civil and Environmental Engineering, London, Ontario, Canada, 80 pages. ISBN: (print) 978-0-7714-2662-9; (online) 978-0-7714-2663-6.

21. Predrag Prodanovic and Slobodan P. Simonovic (2007). Development of Rainfall Intensity Duration Frequency Curves for the City of London Under the Changing Climate. Water Resources Research Report no. 058, Facility for Intelligent Decision Support, Department of Civil and Environmental Engineering, London, Ontario, Canada, 51 pages. ISBN: (print) 978-0-7714-2667-4; (online) 978-0-7714-2668-1.

22. Evan G. R. Davies and Slobodan P. Simonovic (2008). An integrated system dynamics model for analyzing behaviour of the social-economic-climatic system: Model description and model use guide. Water Resources Research Report no. 059, Facility for Intelligent Decision Support, Department of Civil and Environmental Engineering, London, Ontario, Canada, 233 pages. ISBN: (print) 978-0-7714-2679-7; (online) 978-0-7714-2680-3.

23. Vasan Arunachalam (2008). Optimization Using Differential Evolution. Water Resources Research Report no. 060, Facility for Intelligent Decision Support, Department of Civil and Environmental Engineering, London, Ontario, Canada, 42 pages. ISBN: (print) 978-0-7714-2689-6; (online) 978-0-7714-2690-2.

24. Rajesh Shrestha and Slobodan P. Simonovic (2009). A Fuzzy Set Theory Based Methodology for Analysis of Uncertainties in Stage-Discharge Measurements and Rating Curve. Water Resources Research Report no. 061, Facility for Intelligent Decision Support, Department of Civil and Environmental Engineering, London, Ontario, Canada, 104 pages. ISBN: (print) 978-0-7714-2707-7; (online) 978-0-7714-2708-4.